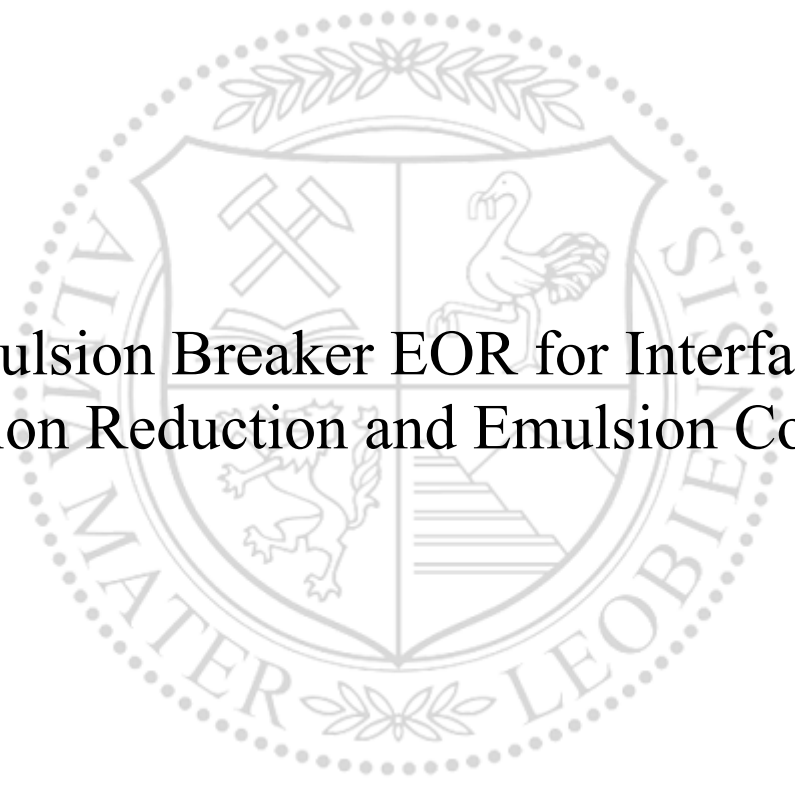




Chair of Reservoir Engineering

Master's Thesis



Emulsion Breaker EOR for Interfacial
Tension Reduction and Emulsion Control

Oscar Rojas Bermudez

September 2019

*Dedicated to my beloved family whom across the distance
supported me with love, advice, and courage.*

AFFIDAVIT

I declare on oath that I wrote this thesis independently, did not use other than the specified sources and aids, and did not otherwise use any unauthorized aids.

I declare that I have read, understood, and complied with the guidelines of the senate of the Montanuniversität Leoben for "Good Scientific Practice".

Furthermore, I declare that the electronic and printed version of the submitted thesis are identical, both, formally and with regard to content.

Date 22.09.2019



Signature Author
Oscar, Rojas Bermudez
Matriculation Number: 11770858

Acknowledgements

I am thankful to my internal supervisor Prof. Holger Ott for his dedication to us during the master courses, and for encouraging us to understand the essence of the physical phenomena taking place in our study field.

In addition, I would like to thank my co-internal supervisor Prof. Riyaz Kharrat, for his insight and advice during the research work.

Further, I would like to express my gratitude to my external supervisor Dr. Christen Knudby. This thesis would not have been possible without his support and interest.

I want to acknowledge RAG Exploration & Production GmbH, for supporting this research. Especially the Reservoir Management Department team.

Finally, it will be not possible to name every person who showed interest and collaborated for the project whit out making the list long. For it, I extend my gratitude to the Montanuniversity staff.

Abstract

During water injection, the driving forces controlling fluid flow in porous media are diverse and include viscous forces, capillary forces, and gravitational forces. At the end of water flooding, the capillary force, which can be related to the residual oil saturation, S_{or} , is the dominant trapping mechanism. This force is the result of the fluid-fluid and rock-fluid interaction. In order to mobilize the residual oil, a significant reduction of capillary force is needed. The interfacial forces (IFT) between two immiscible fluids in a porous media are directly related to capillary forces, and their state of energy can be modified by natural or synthetic surface-active materials. This research project investigated the application of economic, chemically enhanced oil recovery methodologies. The target is to reduce the interfacial energy of the oil-brine system, in a reservoir which can be considered as special due to its interesting characteristics such as low salinity, high reservoir temperature, and importantly, the possible presence of tight emulsions.

During this research, fluid characterization was performed, where the produced mixture containing water in oil emulsions was classified as tight emulsions. The emulsions showed stability at temperatures up to 94 °C and centrifugal forces, as high as 4400 m/s^2 . Since a clear oil-water separation could not be achieved, the emulsified sample was used for screening experiments. The plausibility of Alkali (Sodium Carbonate, $NaCO_3$) application was tested under phase behavior (turbulent conditions) and dynamic interfacial tension (centrifugal force) experiments but discarded due to its limited ability to reduce the interfacial tension. An emulsion breaker solution proved effective at reducing the interfacial tension and thereby breaking the emulsions. Oil droplet morphology deformations were observed during IFT measurements. Ellipsoidal and ballooned droplet shapes appeared under low and high emulsion breaker (EMB) concentrations, respectively. These shapes are hypothesized to be linked not only to the EMB concentration in the brines but as well to the temperature used during the experiment. The demulsifying effect improved drastically with an increase of the kinetic energy in the system (temperature), which enhanced the diffusion of the demulsifier molecules to the interfacial film of the water in oil emulsions. Displacing experiments are needed in order to approve or discard the emulsion breaker application as an EOR agent.

Zusammenfassung

Wenn Sole, ein Gemisch aus Wasser und Salzen, in poröses Gestein injiziert wird, um Erdöl an die Oberfläche zu fördern, wirken verschiedene Kräfte auf das Öl. Diese Kräfte, bestehend aus viskosen Kräften, Gravitationskräften und Kapillarkräften, haben Auswirkungen auf die Strömung des Fluids. Zuletzt bleibt jedoch immer ein Restgehalt an Öl (S_{or}) im Gestein zurück, was auf die Kapillarkräfte zurückzuführen ist. Diese Kräfte entstehen durch die Interaktion der Fluide, Öl und Sole, oder jene von Öl und Gestein. Um das zurückbleibende Öl vollständig aus dem Erdreich zu bekommen, müssen die Kapillarkräfte abnehmen. Die Kräfte, die zwischen zwei nicht mischbaren Flüssigkeiten in porösem Gestein wirken, sind proportional zu den Kapillarkräften und können durch Zugabe von natürlichen oder synthetischen oberflächenaktiven Materialien verändert werden.

Im Rahmen dieser Diplomarbeit wurde die Anwendung der ökonomischen verbesserten Ölrückgewinnung, der Chemischen, untersucht. Ziel der Forschungsarbeit war es, die interagierenden Kräfte eines Öl-Sole-Systems in einem Reservoir, welches besondere Eigenschaften aufweist, zu untersuchen. Speziell dabei waren die hohe Reservoir-Temperatur, der geringe Salzgehalt und die Wahrscheinlichkeit des Vorhandenseins einer stabilen Emulsion. Eine Charakterisierung des geförderten Fluids wurde durchgeführt, bei der sich bestätigt hatte, dass es sich um eine stabile Emulsion von Wasser in Öl handelt, die sich bis zu einer Temperatur von 94 °C und einer Zentrifugalkraft von 4400 m/s^2 nicht trennen ließ. Weiterführend wurde der Emulsion eine Alkalisole (Sodium Carbonate, $NaCO_3$) zugesetzt, um die Grenzflächenspannung zwischen Öl und Lösung zu reduzieren, um in Folge die Emulsion zu trennen. Da dieser Versuch erfolglos blieb, wurde statt der Alkalisole eine Sole mit Demulgator zugesetzt, welche die Spannung erfolgreich reduzieren konnte und somit die Emulsion brach. Während der Spannungsmessungen, wurde eine Deformation der Wasser-Öl-Emulsionstropfen beobachtet. Bei geringer Konzentration des Demulgators bildeten sich ellipsoide, bei hoher Konzentration, runde Tropfen, aus. Die Tropfenform war nicht nur von der Konzentration des Demulgators abhängig, sondern ebenso von der Temperatur. Bei Erhöhen der Temperatur und somit Erhöhen der kinetischen Energie im System verbesserte sich die Entmischung der Öl-Wasser-Phasen.

Table of Contents

| | |
|---|------|
| Declaration | iii |
| Erklärung..... | iii |
| Acknowledgements | iv |
| Abstract v | |
| Zusammenfassung..... | vi |
| Table of Contents | vii |
| List of Figures | ix |
| List of Tables..... | xi |
| Nomenclature | xiii |
| Abbreviations | xv |
| Chapter 1..... | 1 |
| 1.1 Background and Context..... | 2 |
| 1.2 Scope and Objectives..... | 2 |
| 1.3 Thesis Overview | 3 |
| Chapter 2..... | 5 |
| 2.1 EOR | 5 |
| 2.1.1 Chemical EOR..... | 6 |
| 2.2 Interfacial Tension, IFT | 7 |
| 2.2.1 Capillary Number | 8 |
| 2.2.2 IFT and P_c | 9 |
| 2.2.3 Laplace Pressure..... | 9 |
| 2.2.4 Young's Equation..... | 10 |
| 2.2.5 Young-Laplace Equation..... | 11 |
| 2.2.6 Spinning Drop Tensiometer for IFT Determination..... | 11 |
| 2.3 Surface-active Agent Anatomy..... | 13 |
| 2.3.1 Surfactant Head and Tail Energy - Effect on ITF | 14 |
| 2.4 Phase Behavior..... | 15 |
| 2.4.1 Winsor's Ratio..... | 15 |
| 2.5 Natural Emulsions..... | 16 |
| 2.5.1 Natural Surface-Active Agents | 19 |
| 2.6 Demulsification Mechanism | 20 |
| 2.6.1 Emulsion Breaker | 21 |
| Chapter 3..... | 24 |
| 3.1 Spinning Drop Tensiometer Setup..... | 26 |
| Chapter 4..... | 28 |

| | | |
|-----------|--|----|
| 4.1 | Well Sampling | 29 |
| 4.2 | Fluid Separation..... | 29 |
| 4.2.1 | Centrifuge..... | 30 |
| 4.3 | Phase Behavior of Full and Light Fraction Samples..... | 31 |
| 4.4 | Emulsion Characterization..... | 34 |
| Chapter 5 | | 37 |
| 5.1 | Phase Behavior..... | 37 |
| 5.1.1 | Salinity Effect..... | 37 |
| 5.1.2 | Temperature Effect..... | 38 |
| 5.1.3 | EMB – Ambient Temperature Effect | 39 |
| 5.1.4 | EMB – Reservoir Temperature Effect..... | 40 |
| 5.2 | Interfacial Tension Measurements | 41 |
| 5.2.1 | IFT – Distilled Water | 42 |
| 5.2.2 | IFT – Reservoir Salinity | 42 |
| 5.2.3 | IFT – Emulsion Breaker | 43 |
| 5.3 | Discussion..... | 50 |
| 5.3.1 | Ellipsoidal Deformation | 50 |
| 5.3.2 | Ballooning Deformation..... | 52 |
| 5.3.3 | Capillary Number and Sor Reduction | 54 |
| Chapter 6 | | 56 |
| 6.1 | Conclusion | 56 |
| 6.2 | Summary | 58 |
| 6.3 | Future Work..... | 59 |
| Chapter 7 | | 61 |

List of Figures

| | |
|--|----|
| Figure 1. Atoms/molecules at interfaces, bulk and surface atoms generating interfacial energy. | 8 |
| Figure 2. Residual oil and capillary number relationship for different rock types (Lake, 1989). | 9 |
| Figure 3. Representation of an oil drop into water with radius "R". | 10 |
| Figure 4. Schematic representation of oil, water, and solid interactions. | 10 |
| Figure 5. Trapped oil fraction due to capillary forces. | 11 |
| Figure 6. Representation of the Spinning Drop Tensiometer measurement (Krüss, 2019). | 11 |
| Figure 7. Shape parameter corresponding to a given droplet shape for IFT calculation (Dataphysics, 2013). | 13 |
| Figure 8. Surfactant classification based on the hydrophilic head type (W. Lake, 1989). | 13 |
| Figure 9. Surfactant-surfactant interaction at the fluid interface. Red arrows are representing repulsive forces. | 14 |
| Figure 10. <i>Effect of brine salinity concentration on fluid interface phase bending direction.</i> | 15 |
| Figure 11. Schematic representation of the three main types of the Winsor ratio. The three upper diagrams illustrate oil, water, and emulsion phase. The three lower diagrams represent the ternary diagram with the distinction of two- and three-phase system (Lake et al., 2006b). | 16 |
| Figure 12. Schematic representation of a mixture of oil and water, with and without Emulsion Breaker addition (H. Vernon Smit, 1987). | 16 |
| Figure 13. Oil in water emulsions microscopy (Lake, 2006). | 17 |
| Figure 14. Water in oil emulsions microscopy (Lake, 2006). | 17 |
| Figure 15. Complex emulsion, water into oil into water emulsion microscopy (Larry Lake, 2006). | 18 |
| Figure 16. Emulsion size distribution classification, tight, medium, and loose emulsion (Lake, 2006). | 18 |
| Figure 17. Microscope photo of water in oil emulsions stabilized by fine particles (Lake 2006). | 19 |
| Figure 18. Water in Oil emulsion being coated by a negatively charged material at the surface. | 20 |
| Figure 19. Emulsion breakdown by interstitial film destabilization (Lake, 2006). | 22 |
| Figure 20. Schematic representation of the demulsification process of the water in oil emulsions (Ramalho, 2010). | 23 |
| Figure 21. Precision scale from KERN EG. | 24 |
| Figure 22. Testing tubes for Phase Behavior experiments, and capillary tubes for Spinning Drop Tensiometer measurements. | 25 |
| Figure 23. Ultrasonic bath, BADELIN-Sonorex. | 25 |
| Figure 24. Digital microscope VHS-600, KEYENE. | 26 |
| Figure 25. Cooling/heating Julabo CD-200F. | 27 |
| Figure 26. Dataphysics STV-20 components. | 27 |
| Figure 27. Samples A and B after centrifuging at 2000 rpm and 70 minutes @ 23°C. At the top left of each sample the separated emulsion fraction. | 30 |
| Figure 28. Water fraction in samples A (right) and B (left). | 31 |
| Figure 29. Phase behavior of full sample after 48 hours at 60°C. 1) Oil plus distilled water, and 2) oil plus 2.8 g/l NaCl. | 32 |
| Figure 30. Phase behavior of light fraction sample after 48 hours at 60°C. 1) Oil plus distilled water, and 2) oil plus 2.8 g/l NaCl. | 33 |
| Figure 31. The before and after of centrifuging samples A and B. | 34 |
| Figure 32. Micrography of water into oil emulsions contained in sample A. | 35 |
| Figure 33. Sample A emulsions. Emulsion size varying from 1 μm up to 13 μm | 35 |
| Figure 34. Emulsion microscopy from sample A used for emulsion size distribution. Section used denoted by the red dashed lines. | 36 |

| | |
|---|----|
| Figure 35. The emulsion size distribution of sample A showing a normal distribution in the range of tight emulsions..... | 36 |
| Figure 36. Phase behavior - Salinity effect (a) cero, B) 2800 and c) 12000 ppm salinity) on the phases generated in the system. | 38 |
| Figure 37. Temperature effect on phase behavior, A) 24°C B) 60°C, and C) 94°C. It is shown next to figures A and B an emulsion gradient in the samples. Whereas at 94 °C a gradient could not be perceived but a sharp envelope separating oil and the emulsions..... | 39 |
| Figure 38. Phase behavior of systems containing emulsion breaker at different concentrations (50, 76, 131, 190 ppm from left to right respectively) at ambient temperature. | 39 |
| Figure 39. Emulsion breaker concentration variation after 48 hours at reservoir temperature, 94 °C. The red line defines the envelop at which the water-oil interface was allocated at the beginning of the experiment. | 41 |
| Figure 40. Dynamic interfacial tension measurement of Sample "A" vs distilled water, at 6000 rpm. | 42 |
| Figure 41. Dynamic interfacial tension measurement of Sample "A" vs 2.8 g/l NaCl, at 5500 rpm. | 43 |
| Figure 42. Interfacial tension measurements with solutions containing Sample A vs 4.5 g/l NaCl + 18 ppm EMB. | 44 |
| Figure 43. Droplet volume changes with solutions containing Sample A vs 4.5 g/l NaCl + 18 ppm EMB..... | 45 |
| Figure 44. Interfacial tension measurements with solutions containing Sample A vs 4.5 g/l NaCl + 74 ppm EMB. | 46 |
| Figure 45. Droplet volume changes with solutions containing Sample A vs 4.5 g/l NaCl + 74 ppm EMB..... | 46 |
| Figure 46. Interfacial tension measurements with solutions containing Sample A vs 4.5 g/l NaCl + 150 ppm EMB. | 47 |
| Figure 47. Droplet volume changes with solutions containing Sample A vs 4.5 g/l NaCl + 150 ppm EMB..... | 48 |
| Figure 48. Interfacial tension measurements at constant temperature for different EMB concentrations. | 49 |
| Figure 49. Oleic drop morphology variation while interacting at low and higher emulsion breaker concentrations in combination with high temperatures. | 50 |
| Figure 50. Interfacial tension measurement of Sample A vs 4.8 g/l NaCl and 18 ppm EMB, at 3000 rpm. | 51 |
| Figure 51. Ellipsoidal deformation of the droplet along the "Y" axis under low emulsion breaker concentrations. | 51 |
| Figure 52. Interfacial tension measurement of Sample A vs 4.8 g/l NaCl and 150 ppm EMB, at 3000 rpm and droplet morphology change during the experiment. | 52 |
| Figure 53. Droplet horizontal and vertical diameter reduction- increment respectively..... | 53 |
| Figure 54. A) Alpha parameter vs time and B) Width-Hight ratio vs. Alpha parameter. | 54 |
| Figure 55. Capillary number of cases A and B (Lake, 1989). | 55 |

List of Tables

| | |
|--|----|
| Table 1. Field and well characteristics..... | 28 |
| Table 2. Fluid volume and salinity concentration for phase behavior tests. | 32 |
| Table 3. Experimental setup of phase behavior using low emulsion breaker A concentration. | 40 |

Nomenclature

| | | |
|----------|---------------------|----------------|
| N_2 | Nitrogen | |
| $NaCO_3$ | Sodium Carbonate | |
| KCO_3 | Potassium Carbonate | |
| Na^+ | Sodium Cation | |
| pH | Hydrogen potential | |
| v | Fluid velocity | [m/s] |
| μ | Viscosity | [cP] |
| σ | Interfacial tension | [mN/m] |
| γ | Interfacial tension | [mN/m] |
| R | Radius | [mm] |
| Cos | Cosine | |
| θ | Contact angle | [$^\circ$] |
| ω | Angular velocity | [rpm] |
| ρ | Fluid density | [g/cm^3] |
| a | Radius of curvature | |
| α | Shape factor | |
| P | Pressure | [bar] |
| T | Temperature | [$^\circ C$] |

Abbreviations

| | |
|-----------|---|
| RF | Recovery Factor |
| IFT | Inter Facial Tension |
| N_c | Capillary Number |
| S_{or} | Residual oil saturation |
| E.H. | Head Energy |
| E.T. | Tail Energy |
| OIIP | Oil Initially in Place |
| W/O | Water into Oil |
| O/W | Oil into Water |
| C.S.W. | Cayias Schechter Wade |
| EOR | Enhanced Oil Recovery |
| RAG | Rohöl-Aufsuchungs Aktiengesellschaft |
| EMB | Emulsion Breaker |
| P_c | Capillary Pressure |
| SARA | Saturates, Aromatics, Resins, and Asphaltenes |
| PEO | Polyethylene Oxide |
| PPO | Polypropylene Oxide |
| AFM | Atomic Force Microscopy |
| MD | Measured depth |
| PC | Personal Computer |
| Ppm | Parts per million |
| TAN | Total Acid Number |
| T_{res} | Reservoir Temperature |
| cP | Centipoise |

Chapter 1

Introduction

During the last decade's many forms of alternative energy have been arising, and yearly renewable sources contribute gradually more energy to global consumption. However, to date, the oil and gas industry is the leader as an energy provider to the society, mainly due to the oil-gas availability, convenient transport, and the amount of chemical energy contained in it. Nevertheless, conventional petroleum reserves are already in its late productive stage. Then, in order to fulfill the society demands, the challenge had become to be able to extract more efficiently the petroleum from the petroleum reservoirs by increasing the knowledge of the physical phenomena taking place as the reservoir is being produced.

As the energy of an oil reservoir is consumed by extraction activities, a significant fraction of the oil remains at the subsurface. The percentage of oil remaining varies in magnitude and depends on the driving mechanism acting in each reservoir. Even after additional measures have been applied in order to maintain an economical oil production; such as water injection, considerable quantities of oil are still trapped in the reservoir, in some cases in as much as 60 % OOIP (Lyons et al., 2011). In order to increase oil production, one practice is to improve the understanding of the interaction between reservoir fluids and the rock in which they are allocated.

Enhanced Oil Recovery (EOR) involves the introduction of a material/substance that the reservoir has not previously seen. Its objective is to utilize the properties of the injected material to modify the forces that prevent the fluid flow in the reservoir to enhance the field production (Lake, 1989).

1.1 Background and Context

To date, Rohöl-Aufsuchungs AG Exploration and Production GmbH (RAG), has an extensive EOR study covering the Austrian region. However, further research may open a window for the implementation of methodologies that could prove to be economical and provide significant oil recovery incremental. The intention of this research project is to function as an extension of the previous study, for further reservoir description, opportunities detection, and understanding of the Puchkirchen Oil Field.

The north Alpine foreland basin covers a vast region from Geneva to Vienna, all the way through the northern section of the Alps. Within this basin lays the Puchkirchen reservoir, which has been selected for the current thesis project (Limnic series). Several of the oil fields in this region were detected in the Cenomanian and Eocene horizons in the years of 1950s to the present. The reservoirs in these formations such as the Upper Jurassic, Upper Cretaceous (Cenomanian) and Upper Eocene (Voitsdorf Formation) are characterized as highly complex structures, and in most cases compartmentalized (Gross et al., 2015).

The Puchkirchen Field has 64 years of oil production (RAG, 2013), to date the field is being produced via sucker rod pumps, and it is planned to start water injection into the field later this year or in 2020. In addition, the Puchkirchen wells are being treated with additives; such as anticorrosion and demulsifier.

1.2 Scope and Objectives

The objective of this work is to gain a deeper understanding of the reservoir fluids and their possible interaction in the reservoir, and a proper evaluation of Chemical EOR methodologies at laboratory conditions.

Given the equipment available, the oil-brine interactions can be investigated under turbulent conditions (phase behavior), and centrifugal forces (spinning drop tensiometer). These methodologies are used to characterize the actual interfacial energy (IFT) of the fluids, and the IFT change between the oil and synthetic brines. Initially, Alkali EOR was the focus of this research project. The performance of Sodium Carbonate brines ($NaCO_3$) were evaluated at laboratory conditions. After phase behavior and spinning drop tensiometer experiments, the alkali application was classified as to have a limited action regarding the interfacial tension reduction. The reason is attributed to the low total acid number of the Puchkirchen Oils. Then, under this circumstance, the reservoir oil and alkali brine could not achieve a significant interfacial tension reduction. However, the emulsified fluids being produced opened a window for the application of alternative methods. Then, the plausibility of Emulsion Breaker (EMB)

injection/flooding as an EOR method was investigated. The desired effects were to reduce the interfacial tension and to break the emulsions contained in the system simultaneously.

1.3 Thesis Overview

In this section, a quick tour through the contents of the thesis will be provided. The starting point of the thesis is the literature review, and it will briefly cover the background for the understanding of the later chapters.

The literature review (Chapter 2) describes the main categories of enhanced oil recovery available, with an emphasis on chemical EOR. The next section introduces the interfacial energy as it is encountered in nature and its connection to the capillary force that traps the oil in the porous media. Then, the theories which provide the means to quantify the magnitude of the interfacial tension are shown, and finally, the principle of measurement of the Spinning Drop Tensiometer is given. In order to explain how the interfacial energy of a system can be modified, the concept of surface-active agents, and why they can act at the interface of two fluids, is presented. The surfactant anatomy is described, as well as its electrostatic interaction with the oil and brine and the neighboring surfactants at the fluids interface. Consequently, the Winsor's ratio for emulsion classification is shown. This classification will be useful not only due to the phase behavior experiments performed in this research, but also to characterize the emulsion that already exists in the Puchkirchen samples. In order to understand the cause of the emulsions present in the samples, a section which explains the sources of natural emulsion stabilizer material is given. The hypothesized responsible material for emulsion stabilization is discussed, as well as the critical points in which emulsions may be generated by the addition of mixing energy into the system. The last step of the literature review covers how an emulsion is destabilized by the different demulsification mechanisms, and finally, how an emulsion breaker acts to free the water emulsified in the mixture.

Following this track, all the equipment used in this project is showed in Chapter 3, for instance: equipment used for fluid characterization, experimental procedure, chemicals used for brine preparation, measuring devices; such as the Spinning Drop Tensiometer, and the fluids used.

The next chapter covers the field and well characteristics, and the measures taken while sampling the wells to retrieve representative samples for the experiments. The next section leads to the fluid separation to oil and water fractions, and the methods used to try to achieve the separation. Sample characterization by microscopy image is shown, as well as the droplet size distribution derived from the analysis.

Chapter 5 provides the experimental setup, results, and the observations coming from the phase behavior and spinning drop tensiometer experiments. In the discussion section, is reviewed

two main phenomena that were observed during the experiments: a change of the droplet morphology, in the presence of oil and brines containing emulsion breaker at different concentrations, and apparent activation energy that enhanced the interfacial tension reduction and demulsification mechanism.

Finally, Chapter 6 provides the conclusions derived from the project and the observations made during the experiments. A description of recommended future work is given, it briefly provides a set of experiments that can be used to clarify if it is possible to use EMB as an enhanced oil recovery method, or alternatively, to discard it. The last section of the chapter introduces a brief summary of the work done during this research project.

Chapter 2

Literature Review

In this chapter concepts will be briefly presented to understand better the concept of Enhanced Oil Recovery, and how the interactions that take place at the molecular level manifest themselves into a larger scale to enhance the oil production. For it, a walk through the available enhanced oil recovery methods (EOR) is given, as well as the driving mechanisms and the physics that builds up the logic for the use of Emulsion Breaker in this research project.

2.1 EOR

A good starting point is by having a global understanding of what does EOR mean and what effect on oil production has. But first, the production phases of an oil field will be reviewed.

Primary production corresponds to the drainage due to the natural energy of the reservoir. This natural energy is classified into a set of drive mechanisms; such as fluid-rock expansion, solution gas, aquifer influx and gas cap (in most cases RF=19% but varies depending on the reservoir rock-fluid and or aquifer properties) (Ott, 2018a). Secondary recovery aims to assist against the natural pressure decline of the reservoir to maintain a reasonable production, hence, water injection or immiscible gas injection (N_2) comprises the most common tools for maintaining reservoir pressure.

EOR, in short words, refers to the action of exposing the reservoir to materials that were not previously present in the reservoir (Lake, 1989). Lately, most of the interest has been placed on EOR (Lake, 1989). The envelope that defines the line of whether a recovery method is or is not an EOR lays on the capacity of the injected material to change the petrophysical properties of the reservoir rock and the fluids contained in it. Several EOR methods are available, but they can be catalog mainly as Thermal, Gas, and Chemical methods. Chemical EOR is the focus of this thesis.

2.1.1 Chemical EOR

Chemical EOR includes mainly Surfactant, Polymer, Alkali, and Low-Sal injection. Each methodology targets the increase of the oil recovery by different means, and their effects can be summarized as follows:

Polymers: Polymers increase the viscosity of the displacing fluid (injected fluid) to improve mobility ratio and hence sweep efficiency (Sheng, 2013b).

Surfactants: Surfactants lower the interfacial energy, IFT, between fluids, which leads to a reduction of the capillary pressure. As a result, the trapped phase at the porous media becomes movable (Shah, 2012).

Alkali: Alkali has the same effects as the ones perceived in the surfactant application but in a lower magnitude (Sheng, 2013a). The main difference is that alkali is used to generate surfactants in situ, as opposed to injecting them.

Low Salinity: The effects of Low-Sal have shown in different cases a change of wetting state of the rock. From oil-wet to water-wet in carbonates. In Sandstones it is reported clay swelling, fines migration, and due to the high pH of the solution, Low-Sal acts like alkaline flooding (Sheng, 2013c).

The use of **Emulsion Breaker** as an enhanced oil recovery method has not been reported yet. Still, the anatomy and nature of an emulsion breaker are in principle the same as that of a surfactant. Therefore, the surfactant background is useful to understand an emulsion breaker action.

2.1.1.1 Surfactants Background

The first idea that may appear when the term surfactant is brought on to the table is expensive. No wonder arises into having this first impression, and no blame is given since surfactant projects have always been accompanied by significant monetary investments and intensive laboratory research. Hence, the first desire in this work is to clarify what is a surfactant, what it does, and the ways that one can encounter them in the industry and in nature.

Chemically speaking, a surfactant is a compound that can be generated by the reaction of water-insoluble fatty acids with an alkali metal (or organic base), to produce a carboxylic acid salt with an enhance in water solubility (Myers, 2005b). Alkali soaps were generated for centuries using animal fats and ashes of wood and plants containing potassium carbonate, K_2CO_3 , to produce a neutral salt. As the mixture was boiled with water, surfactants could be generated. This method was used until the first world war, in which Germany became the first country to develop surfactants for general application. The desire to overcome shortages in available

animal and vegetable fats pushed the development. Their materials were short-chain alkyl-naphthalene sulfonates which came by the reaction of propyl or butyl alcohol with naphthalene followed by sulfonation (the action of the surfactant was marginal but represented a milestone for the surfactant industry) (Myers, 2005b).

Surfactants widely studied, well known and are broadly applied in many fields. The reason is their ability to change the energy of the interfaces. But, before it is discussed how to modify the interfacial energy of a system, it must be reviewed first what is the interfacial energy, and the reason of the existence of this energy at the interface of two immiscible fluids.

2.2 Interfacial Tension, IFT

As seen in nature, when two immiscible fluids; i.e., oil and water, are brought together, an interface that separates the fluids will develop. They separate due to incompatibility of intermolecular interactions between the polar molecules of water and the non-polar molecules of the oil. One could just say that they do not like to interact with each other (Myers, 2005b). The reason is attributed to the asymmetric forces that are encountered at the interface of two immiscible fluids. The root of the asymmetric force lies on the nature of the intermolecular interactions of the polar components and non-polar components. Meanwhile, polar components interact by dipole-dipole interactions; the non-polar components interact by London dispersion force (Calmes et al., 2019). In short, electrons in a polar molecule will spend more time on one side of the molecule, this due to a difference in electronegativity of the atoms that comprise the molecule. As a result, one extreme is positively charged and the other negatively charged (dipole). For a non-polar compound, the electronegativity of its components is almost equal, then the attractive and repulsive force vectors of the molecule are canceled out, creating a more even distribution of its electrons in the molecule. This is what makes the molecule non-polar. However, it is possible that at some point electrons travel to one side of the atom for a short time, creating an instantaneous dipole molecule. The interactions between instantaneous dipole molecules are what is known as London dispersion or Van der Waals Force (Calmes et al., 2019).

Due to this incompatibility of attractive-repulsive forces, the atoms or molecules at the interface will experience higher potential energy than the ones in the bulk of the fluid (Myers, 2005a). This means that at the interface, the molecules of the fluid will interact actively with identical molecules at the bulk rather than the neighboring molecules of the other fluid at the interface (Figure 1). Then, accordingly to thermodynamics, the system will demand an adjustment of the system energy and will reach a minimum surface area (minimum-energy rule) or asymmetric

interactions (Myers, 2005a). At the interface, the energy of a given system is determined by typical characteristics such as pressure and temperature, and the different fluid compositions.

It is important to denote that the interfacial tension of a given system can be significantly changed by small changes in the bulk composition. Hence, the interface energy can be manipulated in such a way that it can be brought into a lower or higher state of energy (Myers, 2005a).

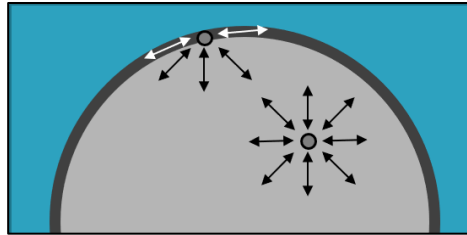


Figure 1. Atoms/molecules at interfaces, bulk and surface atoms generating interfacial energy.

The reduction of the interface energy is of particular interest in the oil industry due to it can be directly related to the fraction of oil that remains trapped in the reservoir rock due to capillary forces. However, capillary force is not the only force dictating the fluid flow at the porous media; a battle of forces takes place in the reservoir as it is being produced. The viscous forces which try to displace the fluids towards the producing well, and the capillary forces which mainly traps the fluids in the reservoir rock.

2.2.1 Capillary Number

The Capillary Number, N_c , provides an idea of the energy balance in the system (Eq. 1). The capillary number is a practical tool (dimensionless) to have a glance of the dominating driving force in the reservoir.

$$N_c = \frac{\text{Viscous Forces}}{\text{Capillary Forces}} = \frac{v \mu}{\sigma} \quad \text{Eq. 1}$$

Where v is the velocity and μ the viscosity of the displacing fluid and σ the corresponding IFT between the displacing and displaced fluids.

One can deduce then, that when the viscous force is higher than the capillary forces the oil gets mobilized towards the producer well, either by water injection or the influx of an aquifer. This is especially true at the immediate vicinity of an injection well, where a high velocity of the injected brine is present. However, as the injected brine finds its way moving deeper through the reservoir, its velocity decreases gradually. There, where the viscous forces have reduced low enough other forces start to manifest. The capillary force becomes evident at low fluid velocities. It is at this point in which the capillary forces keep the oil trapped in the porous

media (Lake, 1989). Experimental investigations show how can be reduced the residual oil saturation of different rock types, i.e., after a water flooding stage (Figure 2). Then, the desaturation of the rock is possible by increasing the capillary number in several orders of magnitude, which at the same time also depends on the pore size and its distribution for a given porous media (Lake, 1989).

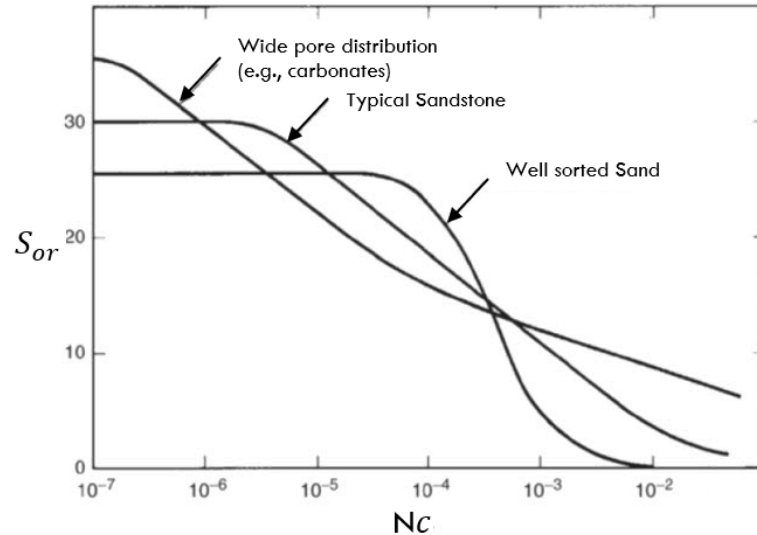


Figure 2. Residual oil and capillary number relationship for different rock types (Lake, 1989).

2.2.2 IFT and Pc

It has been mentioned in the last two sections the interfacial tension and the capillary pressure. One may perceive by now that they are intimately related to each other. Let us try to clarify the connection between these two concepts. For it, it will be related the interfacial tension to the capillary pressure, P_c .

2.2.3 Laplace Pressure

The Laplace pressure for the pressure inside of a sphere (Eq. 2) as defined by Young-Laplace equation, can be used to perceive how a reduction of the interfacial tension is related to a capillary pressure reduction.

$$P = \frac{2\sigma}{R} \quad \text{Eq. 2}$$

Where P is the pressure, σ the interfacial tension between the two fluids and R the radius of curvature of the sphere.

It expresses how the pressure of a fluid drop immersed in another is affected, i.e., an oil droplet submerged into water (Figure 3). It can be concluded by the last equation, that the smaller the

radius of curvature the more prominent the pressure inside the drop, or in the opposite side, the greater the IFT of a given system the higher the pressure inside of the drop (Butt et al., 2003).

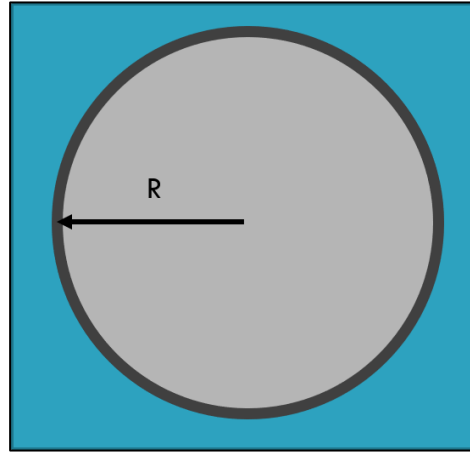


Figure 3. Representation of an oil drop into water with radius "R".

2.2.4 Young's Equation

Additionally, Young's equation (Eq. 3) expresses the rock-fluid forces when the system is at equilibrium. It provides a first glance of the wettability of the system as well. It is based on the relative value of the surface tension of each pair of the three phases. Each surface tension acts in its corresponding interface and the defined angle θ at which the liquid contacts the surface (Figure 4). This is known as the wetting angle of the liquid to the solid in the presence of gas (Morrow et al., 2017).

$$\gamma_{F1S} = \gamma_{F2S} + \sigma_{F1F2} \cos \theta \quad \text{Eq. 3}$$

Where γ denotes surface/interfacial tension between rock-brine, rock-oil and oil-brine as γ_{F1S} , γ_{F2S} and σ , respectively.

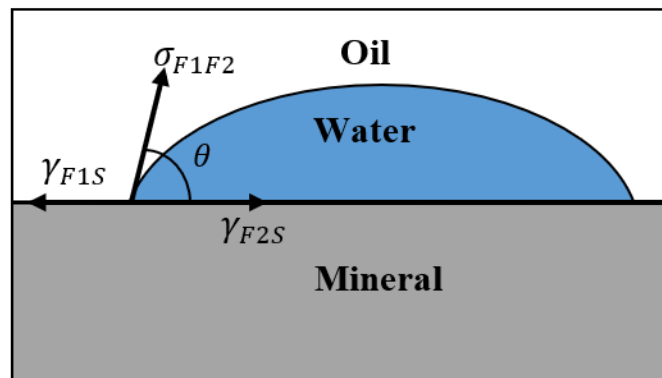


Figure 4. Schematic representation of oil, water, and solid interactions.

2.2.5 Young-Laplace Equation

The Young-Laplace equation results from the combination of the Laplacian equation (Eq. 2) with Young's equation (Eq. 3). The resulting formulation (Eq. 4) expresses the interfacial tension relation to the capillary forces. In addition, a visual representation of an oil fraction trapped by capillary forces is shown in Figure 5.

$$P_c = \frac{2\sigma_{F_1F_2}\cos\theta}{R} \quad \text{Eq. 4}$$

Where P_c is the capillary pressure, σ the interfacial tension between the fluids, θ the contact angle, and R the radius of curvature. By analyzing the last equation becomes more evident that lowering the IFT between the fluids, a direct reduction of the capillary forces is expected.

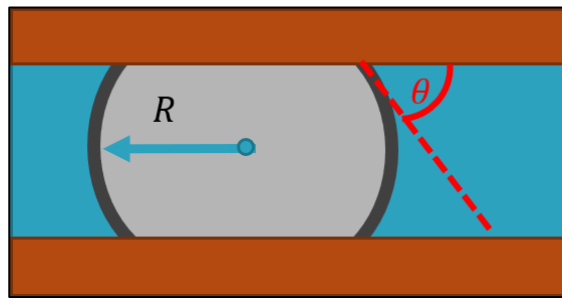


Figure 5. Trapped oil fraction due to capillary forces.

2.2.6 Spinning Drop Tensiometer for IFT Determination

In this thesis, a spinning drop tensiometer was used to characterize the interfacial forces between fluids. This section will briefly cover the theory behind this methodology.

The spinning drop method is an experiment that is used to measure the surface and interfacial tension between two immiscible fluids. It is done by measuring the shape of a drop (gas or liquid) in a denser fluid while rotating in a capillary tube (Figure 6) (Krüss, 2019).

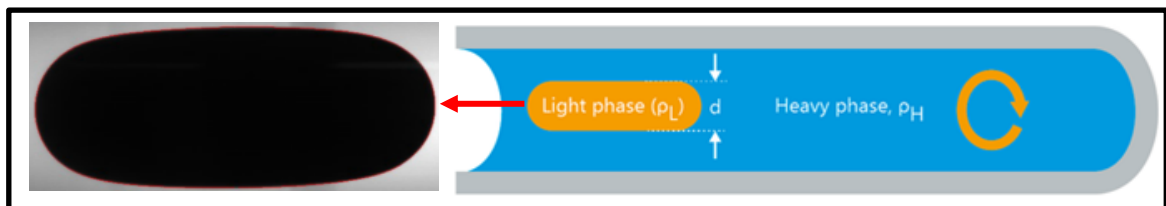


Figure 6. Representation of the Spinning Drop Tensiometer measurement (Krüss, 2019).

The system can be considered in steady-state when a balance between centrifugal and interfacial forces has been reached. Under this circumstance, the drop which spins inside of the capillary tube will stop its deformation. Then, the Lagrangian condition is applied, and the computation of the interfacial tension can be performed (Eq. 5) (Couper et al., 1983).

$$\sigma = \frac{\Delta\rho \omega^2 R^3}{4} \quad \text{Eq. 5}$$

Where $\Delta\rho$ is the density difference between the fluids contained in the capillary tube, R the radius of the drop cylinder, and ω the angular velocity.

It is essential to mention that the method is especially true when the shape of a drop separates from a sphere and approximates a cylindrical shape. Vonnegut's approach theory was proven by D. K. Rosenthal et al., 1962 by full-shape droplets analysis. If one links the pressure difference to the forces applied and using differential equations, like Princens (Arnold, 2018), to fit the profile of a droplet, we can achieve the following equation:

$$\gamma = \frac{\Delta\rho \omega^2}{2\alpha} a^3 \quad \text{Eq. 6}$$

Where a is the radius at the cap and α the shape factor.

J. L. Cayias, R.S. Schechter, and W.H. Wade developed a method in which a more accurate approximation to the interfacial tension of the system could be reached. The theory relies on measuring both the vertical diameter and the horizontal diameter of the drop instead of just one or the other (Cayias et al., 1975). Both methods apply the same formula, but the key in the calculation is the determination of the shape parameter as an iterative calculation procedure (Arnold, 2018).

If one assumes both diameters approaches or equals to ratio 1, it would mean that the drop topology approximates to a sphere shape, which is translated to a system which minimizes its surface area due to high interfacial forces (Figure 7) (DataPhysics, 2013). By the other hand, if the horizontal-vertical diameter ratio changes being the horizontal considerably more significant than the vertical diameter, then it would mean that the drop moved from the spherical shape to approach a more cylindrical shape, the less sphericity of the drop, the higher the surface area and hence the lower the IFT. Moreover, the showed function is exponential, and above the ratio of 4, the changes in the shape parameters become neglectable. Hence it is assumed as a constant value of 16/27 (Arnold, 2018).

Until this stage, it has been reviewed what the interfacial forces are, what controls them, and how to calculate them. The next section will be dedicated to explaining how the interfacial forces can be modified by surface-active agents.

2.3.1 Surfactant Head and Tail Energy - Effect on ITF

Due to the duality of a surfactant, it tends to allocate at the interface and create oriented monolayers. The surfactant head towards the aqueous phase and the tail at the oleic phase.

Both components head and tail, contains electrostatic charges, such that when a pair of surfactant heads or tails with the same charge come closer, repulsive forces will act to separate them, i.e., two magnets that repulse when the same positive or negative poles are brought together. If the energy of a surfactant head, E.H., and the energy of the tail, E.T., are in equilibrium ($E.H. = E.T.$) then the interface will be straight (Figure 9). Moreover, the energy of the head is being affected by parameters such as head type, brine salinity, and co-solvent. Whereas, the tail energy is influenced by the tail length, oil type, oil composition, and co-solvent (Ott, 2018b).

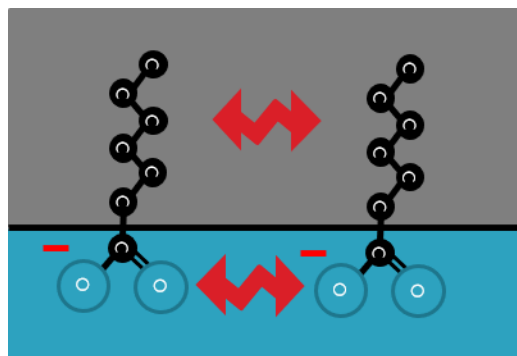


Figure 9. Surfactant-surfactant interaction at the fluid interface. Red arrows are representing repulsive forces.

As mentioned, the brine salinity plays a significant role in the interfacial tension magnitude, and it is used as a tuning parameter. Experimental investigation showed that when brine salinity is increased, an energy bridge is generated. If we assume the presence of negatively charged heads (anionic surfactants), then, the sodium cations (Na^+) will be allocated between two anionic surfactant heads, and therefore the repulsive forces will decrease. Hence, if salinity is increased, the fluid interface will be deformed towards the brine phase (Figure 10-A). On the other hand, if salinity is reduced, the repulsive forces will override the repulsive tail force. As a result, the interface will bend towards the oleic phase (Figure 10-C). Finally, there is an optimum salinity concentration in which the interface will be flat. For us, this is the optimum concentration that is desired to be achieved (Figure 10-B)(Ott, 2018b).

The effect of salinity on the interface topology can be related directly to the Young's Laplace equation. It was previously mentioned, the smaller the radius of curvature, the greater the pressure inside of a bubble and hence the capillary pressure.

The bending direction of the interface, i.e., at high or low salinity will dictate the emulsion type of the system, either water into oil emulsions (W/O) or oil into water emulsions (O/W). Then

when an optimum concentration is achieved, a third microemulsion phase is generated. In order to find the optimum salinity concentration phase behavior tests can be performed to observe how the system will behave at different conditions.

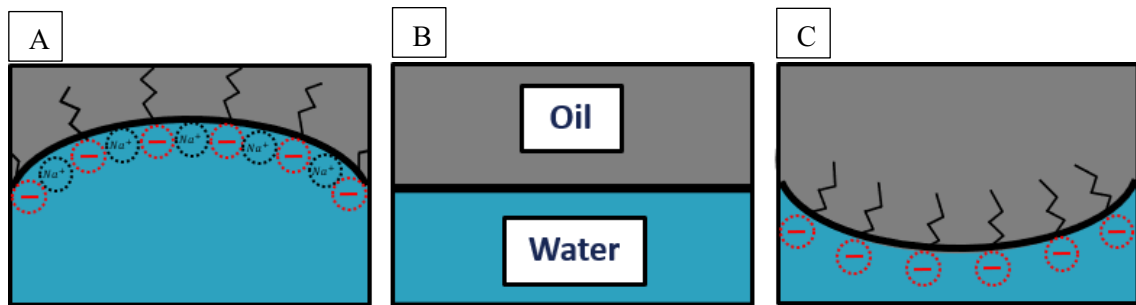


Figure 10. Effect of brine salinity concentration on fluid interface phase bending direction.

2.4 Phase Behavior

The phase behavior of a single fluid can be as complex as its composition. Hence, it is not a surprise that when two more phases are added into the system, the whole complexity increases. However, the phase behavior of a three-phase system is not a new topic and had been investigated over the decades. The first researcher to generate a detailed study of the phase behavior of microemulsions was P. A. Winsor (Winsor, 1948). He found different equilibrium states that a mixture may achieve when water (or a salty aqueous solution) is mixed with a non-polar solution (oil), and enough quantities of surfactants are aggregated.

In fact, up to date, his classification is still used, and it is known as the Winsor's ratio.

2.4.1 Winsor's Ratio

Winsor (1948) found that the phase behavior between an aqueous solution, oil and surfactants could be characterized as belonging to one of three main categories: type II (-), II (+) and III. Types II (-) and II (+) refer to a system in which two phases can be encountered, whereas one can find three phases in a type III category. The positive and negative signs of the type II categories refer to the tie line slope in the ternary diagrams (Figure 11). Based on the diagrams one can see that the Winsor's ratio II (-) and (+) represents the oil into water emulsions (Figure 11-A), and water into oil emulsions (Figure 11-C) respectively.

Interestingly, the surfactant concentration has a lower effect on the phase behavior of the system when compared to the effect that comes by temperature, brine salinity, and hardness. Hence,

salinity can be used as a tuning parameter to achieve the third phase in the system (Figure 11-B)(Lake et al., 2006b).

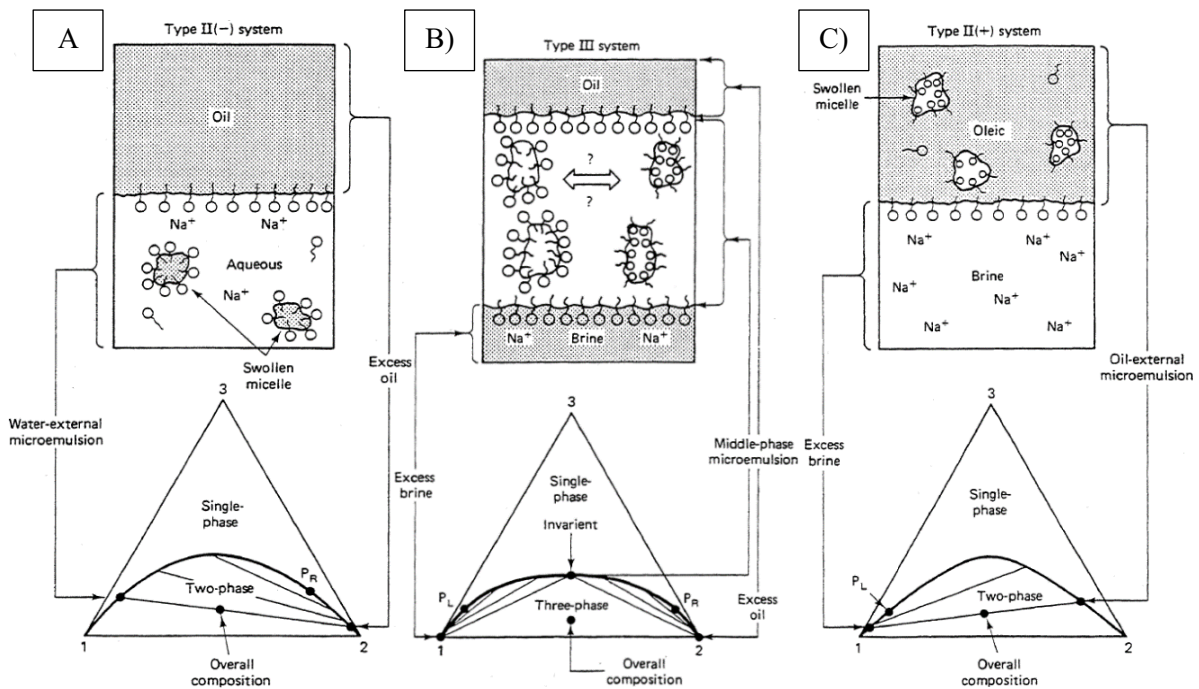


Figure 11. Schematic representation of the three main types of the Winsor ratio. The three upper diagrams illustrate oil, water, and emulsion phase. The three lower diagrams represent the ternary diagram with the distinction of two- and three-phase system (Lake et al., 2006b).

2.5 Natural Emulsions

It was reviewed how surfactants act on the interface, and depending on the energy balance between the head-tail of the surface-active agent, a system may develop different emulsion types. This section will address where natural emulsions may create in the system and the surface-active agents found in nature that stabilizes the emulsions.

After the oleic mixture is produced from the well, the oil must be separated from the water to be shipped, piped, or stored.

If the separation is slow, the production rate may be affected as well (Figure 12).

Usually, the separation lasts from minutes to several hours when the fluids are set at rest. The situation changes when inside the system exists natural emulsion

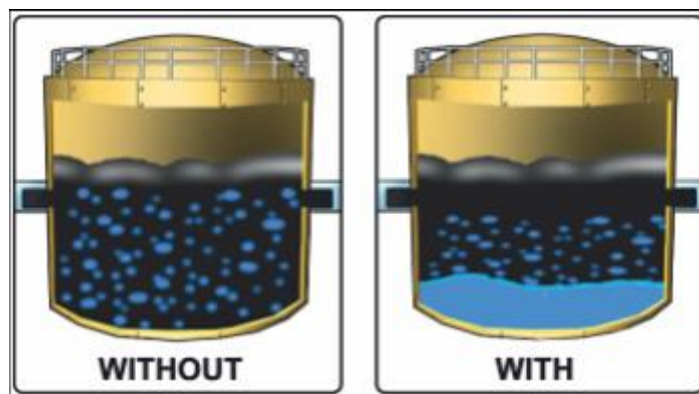


Figure 12. Schematic representation of a mixture of oil and water, with and without Emulsion Breaker addition (H. Vernon Smit, 1987).

stabilizers, and if it is the case, the separation time jumps dramatically.

As literature relates, emulsions can be generated by adding surfactants into the system, either synthetic or in-situ generated, i.e., by adding alkali. However, emulsions are not generated just by the addition of surfactants. First, enough mixing energy must be provided, and an emulsion stabilizer must be present in sufficient quantity. The mixing energy can be found in different points that the reservoir fluids will face as they travel up to the surface. This mixing energy is encountered as the fluid flows through 1) the formation, 2) the sandface and the perforation channels, 3) bottom-hole pump, 4) tubing, 5) choke, 6) and surface equipment (Smit, 1987).

In order to treat emulsions, the first step is to characterize the emulsion in the system and find out what may cause the stabilization of the emulsion. Figure 13 and Figure 14 shows the two basic types of emulsions: water into oil, and oil into water emulsions, being the first the dispersed phase into the continuous second phase.

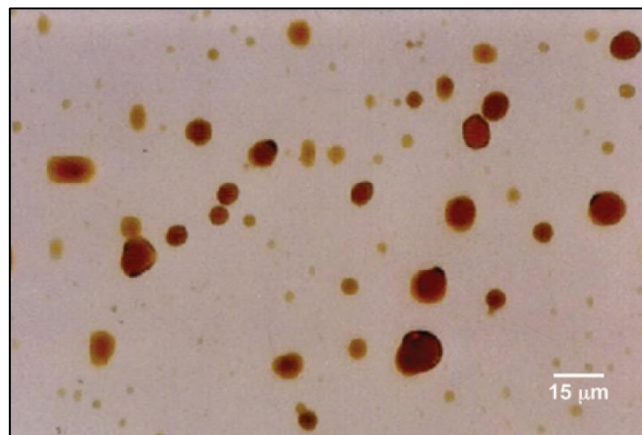


Figure 13. Oil in water emulsions microscopy (Lake, 2006).

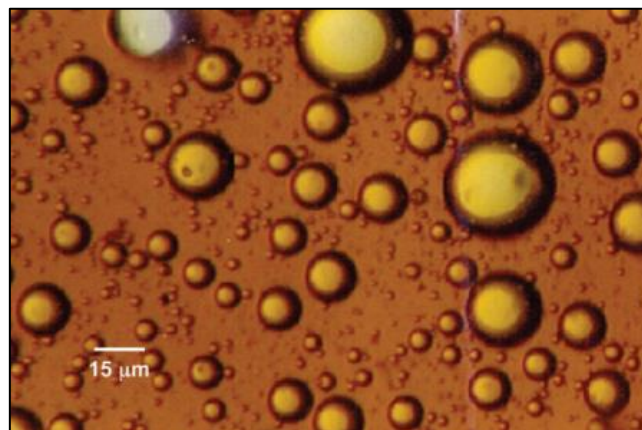


Figure 14. Water in oil emulsions microscopy (Lake, 2006).

Another type of emulsions have been previously reported, and it is known as complex or multiple emulsions, the complexity of this emulsions is greater than the two primary classifications. In this category of emulsions, one can encounter emulsions inside of a dispersed emulsified liquid, i.e., water into oil into water emulsions (Figure 15). As previously mentioned,

the formation of an emulsion depends on several factors. But as a rule of thumb, when the volume of one phase is considerably smaller than the other, the phase in a smaller concentration will be dispersed into the one of greater fraction magnitude.

As a rule of thumb, the higher the mixing energy, the smaller the emulsion size and

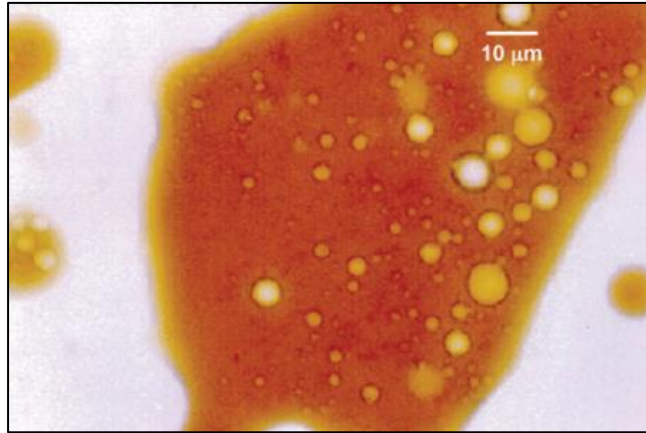


Figure 15. Complex emulsion, water into oil into water emulsion microscopy (Larry Lake, 2006)

consequently, the more stable they become. After mentioning the last, emulsions are also classified by the droplet size and their distribution in the continuous phase. When the emulsion size is bigger than $0.1 \mu\text{m}$ one can refer to them as macro-emulsions. Macro-emulsions are further classified depending on their size distribution into tight emulsions, medium emulsions and loose emulsions (Figure 16). Previous studies have shown that the water droplets can vary from $1 \mu\text{m}$ to as much as $1000 \mu\text{m}$ (Lake et al., 2006b). The factors affecting the drop size distribution of emulsions include IFT, shear, type, and quantity of surface-active agents, presence of solids, and finally, the fluid properties of oil and water.

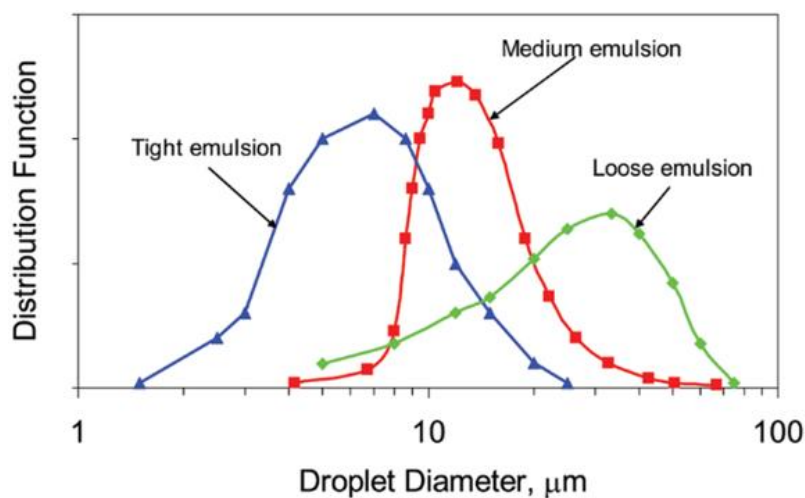


Figure 16. Emulsion size distribution classification, tight, medium, and loose emulsion (Lake, 2006).

2.5.1 Natural Surface-Active Agents

Excluding commercial surfactants or chemically induced surfactants; such as alkali, to date, two main hypotheses of emulsion stabilizer agents have been proposed. A surface-active compound is a molecule that is partially soluble into oil and partially soluble into water. This duality essence can be found after the oleic mixture have been produced, and no water separation had happened (after long periods of time). Hence, some material must prevent the coalescence of the droplets. As literature relates, some emulsifier agents are believed to be **fine particles** and **asphaltic in nature**.

Fine Particles. These fine particles are oil-wet solids such as sand, silt, shale particles, crystallized paraffin, waxes, iron, zinc, aluminum sulfate, calcium carbonate, iron sulfide and materials that can be allocated at the oil-water interfaces and act as an emulsion stabilizer. Hence, the parameters dictating the emulsification by fine particles are 1) particle size significantly smaller than the emulsion drop size, 2) interparticle interaction, and 3) the wettability of the particle (Smit, 1987). The microscope photo in Figure 17 shows the presence of solids in the system (Lake et al., 2006b).

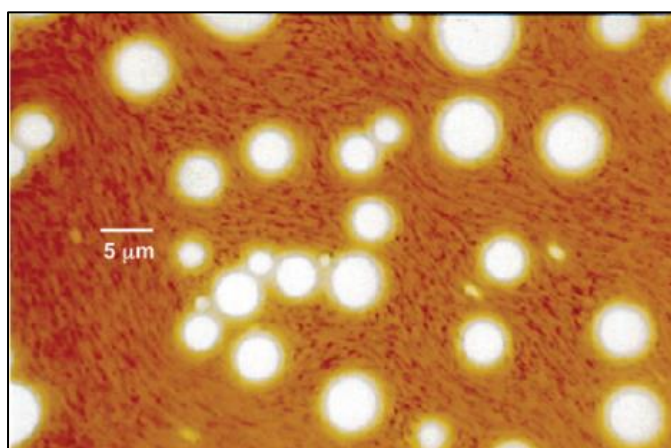


Figure 17. Microscope photo of water in oil emulsions stabilized by fine particles (Lake 2006).

Asphaltic in nature. Extensive research has been conducted regarding W/O emulsions by asphaltenes action where at ratios of approximately 1:1 of asphaltene-resin, emulsions can be generated (Schorling et al., 1999). The resins are the oil fractions insoluble in propane but soluble in n-pentane and n-heptane. Asphaltenes are defined as the insoluble fraction in high polar light n-alkanes, i.e., n-pentane or n-heptane, but soluble in low polar solvents such as toluene and benzene. Asphaltenes can be distinguished by having attached aromatic rings carrying aliphatic rings that contains some polar components like sulfide, aldehyde, carboxylic, and some metals like nickel, vanadium, and iron. These are the components that provide the hydrophilic part to the molecule. Moreover, it has been shown that resins have an analogical structure to the one perceived in asphaltenes, but they are smaller molecules with weaker

interactions at the fluid interfaces. Additionally, it is theorized that resins solvate the asphaltenes macromolecules into smaller asphaltene aggregates. Then, the asphaltene can be allocated at the oil-water interface to stabilize the water drops (Ramalho et al., 2010). Moreover, the asphaltene coating at the interface, in the form of a monolayer, prevents the droplet coalesce by electrostatic forces, as shown in Figure 18. For example, one could imagine two magnets that are brought together from the same polar side; then, due to an incompatibility of the electrostatic interactions, the magnets will repel to each other.

Mingyuan et al., 2006 observed that emulsion stability is a function of the aromaticity, type of functional group in the asphaltenes, and the molecular size of the fractions. Further research performed by Schorling et al., 1999, showed that the ratio between resins and asphaltenes plays a significant role in determining emulsion stability. They concluded that as the resin/asphaltene ratio approached to 1:1 the emulsions on the system emulsions exposed smaller sizes and hence became more stable (Schorling et al., 1999).

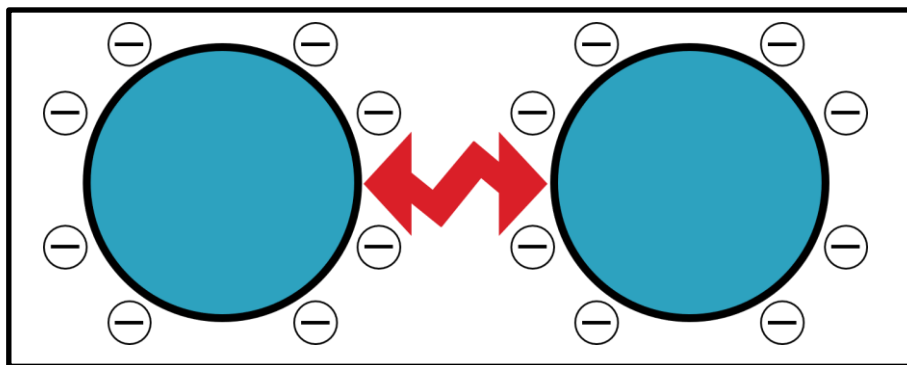


Figure 18. Water in Oil emulsion being coated by a negatively charged material at the surface.

2.6 Demulsification Mechanism

There are several hypotheses of how emulsions can be destabilized, and some authors like Larry Lake explains how emulsions can be broken. The principle lays on the destabilization of the interfacial film that keeps the emulsions in the system (Lake et al., 2006a). Some of the proposed mechanisms are mainly 1) temperature, 2) agitation and shear, 3) solids removal, and 4) control of the emulsifying agent. It will be reviewed in short words, how each mechanism contributes to the destabilization of the emulsions.

1) **Temperature:** The temperature has a direct impact on the intrinsic properties of the mixture. As the temperature goes up, the viscosity of the oil reduces increasing the mobility of the water droplets to be able to achieve a faster settling time. As a consequence, drop collision and coalescence happens more frequently. The temperature increase affects the volume of the water, and due to thermal expansion, the film at the interface will lack enough stabilizing material. It

is imperative to mention that the drawback of this method is the risk of volatilizing the short-chain hydrocarbon molecules when the mixture is heated.

2) **Shearing/agitation:** The reduction of the mixing energy can mitigate the emulsion stability. As mentioned, shearing causes violent mixing regiments, which are translated into smaller droplet sizes. Still, in order to break the emulsions with additives such as emulsion breaker some mixing energy must be provided.

3) **Solids removal:** It refers to prevent the stabilization of emulsions by fine particles. If the solids can be removed directly from the source, then the situation is solved. The solids can be mitigated by dispersing them into the oil, if they are water-wet, then by dissolution in water it can be removed as well.

4) **Control of emulsifying agent:** It targets the careful selection of the injected chemicals during production, due to the backflow of the injected fluids to the formation may generate emulsions. Chemicals such as acids, additives during acid treatments, corrosion inhibitor, surfactants, organic and inorganic deposition control, polymers, and blocking agents. But it also includes oil co-production, this means that producing two incompatible oils will induce solid precipitation of both organic and inorganic particles. i.e., a mixture of asphaltic and paraffinic crude oil will result in asphaltene precipitation. It is recommended to perform compatibility tests in the laboratory prior to production activities (Lake et al., 2006b).

Emulsions can be chemically destabilized, for it demulsifies are being used. A surfactant such as an emulsion breaker has the ability to act on the stabilizer material in order to remove them from the film that has been created around the droplet. In theory, the emulsion breaker molecule has a higher surface activity than the stabilizing material (Allen et al., 1989).

2.6.1 Emulsion Breaker

An Emulsion Breaker or demulsifier is a common additive used in the oil industry, which provides a faster separation of oil and water. Emulsion breakers are prepared as a mixture of active agents commonly known as demulsifier bases which are dissolved into organic solvents like xylene, toluene, short-chain alcohols, and aromatic naphtha. From them, the most used emulsion breakers are poly (ethylene oxide-b-propylene oxide) (PEO-b-PPO) copolymer. These macromolecules expose amphiphilic behavior (polar duality). Moreover, the two types of emulsion breaker Polyethylene Oxide, PEO, and polypropylene oxide, PPO, are also characterized by their hydrophilicity. The PEO chains are more hydrophilic and interact in greater magnitude with polar molecules. Meanwhile, PPO chains are more hydrophilic, therefore, will interact mainly with non-polar molecules (Ramalho et al., 2010).

The Marangoni-Gibbs effect is the most widely accepted explanation of the emulsion stabilization, and it is theorized that when two water droplets approach to each other, a thin interstitial liquid film forms between the two droplets. Then, by capillarity, the fluid is drained out of the film carrying with it some of the adsorbed surfactant molecules out of the interface. As a result, a tension gradient is generated at the interface, being lower tension out of the film and higher inside. Due to the lower concentration of surfactant in the interstitial film, a reverse flux is generated in order to maintain the surfactant concentration at the interface, then the interstitial film thinning stops (Figure 19). In short words, it is a mass transfer along within the interface of two immiscible fluids due to an interfacial tension gradient, from the higher surfactant concentration to the lower surfactant concentration.

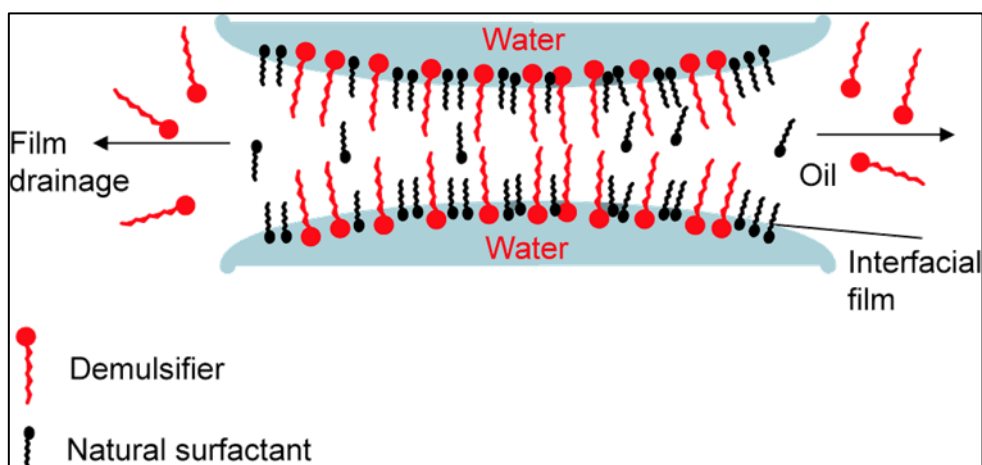


Figure 19. Emulsion breakdown by interstitial film destabilization (Lake, 2006).

The coalescence will take place within the thinning and drainage of the interstitial film. Figure 20 shows the theorized process of demulsification, a) demulsifier passes between the stabilizer material, b) the demulsifier starts to be adsorbed at the interface, c) the aggregates are displaced from the interface, and d) the droplets coalesce (Ramalho et al., 2010).

Mohammed et al., 1993 reported that the emulsion breaker enhances the film thinning by minimizing the tension gradient at the interface. Ese et al., 2000 based on atomic force microscopy, AFM, suggested that a demulsifier provides a similar behavior as the one of resins to asphaltenes. The AFM showed open structures regions when 100 ppm of emulsion breaker was added (Ramalho et al., 2010). Moreover, the effect of emulsion breaker that has on the interfacial energy had been reported as to induce a reduction of the interfacial elasticity, and also of interfacial tension to values down to 0.5 mN/m (Kang et al., 2006).

An emulsion breaker must be correctly selected to suit the specific combination of formation water and oil composition, having mentioned the last one can conclude that the emulsion breaker selection can be as complex as the systems in consideration. Hence, a demulsifier may not perform adequately in every tested emulsified system (Kang et al., 2006).

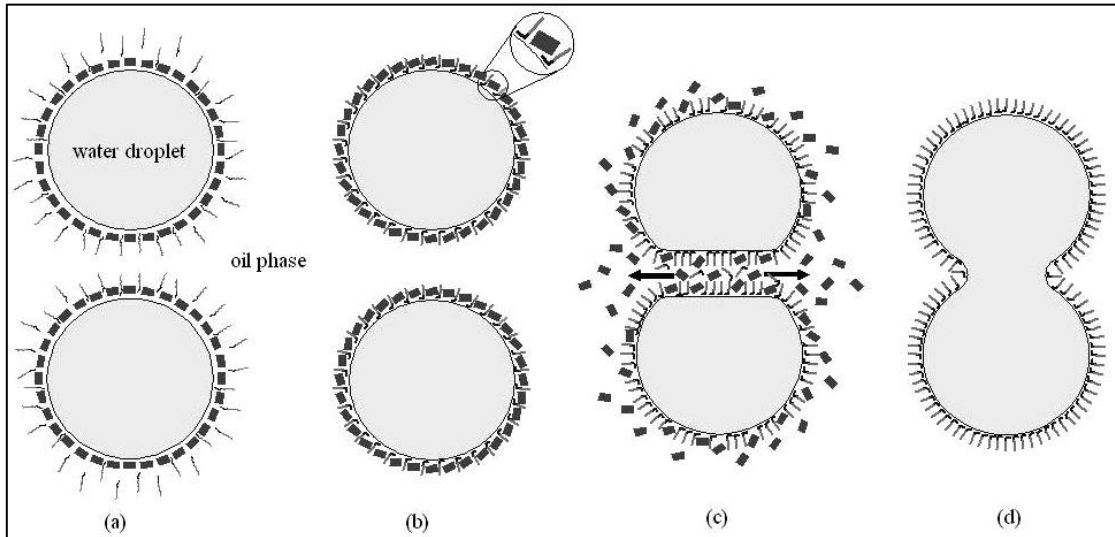


Figure 20. Schematic representation of the demulsification process of the water in oil emulsions (Ramalho, 2010).

Chapter 3

Materials and Equipment

This section will introduce the chemicals, laboratory equipment, and measuring devices used in the project.

The brines used in this project consisted of:

- Sodium **Chloride** (NaCl).
- A demulsifier DMO-86102 supplied by RAG labeled in this thesis as **EMB**, which is developed by Baker Hughes.
- The oil used for experiments is **sample A** as retrieved from the wellhead.
- Distilled Water

In the Puchkirchen Oil field, the demulsifier is currently used at surface conditions in the fluid separator. The sodium chloride and EMB were dissolved/dispersed into **distilled water** in different concentrations to achieve the desired solution, and the quantities dissolved in the brines were weighted by a precision scale (Figure 21).



Figure 21. Precision scale from KERN

EG.

The equipment for phase behavior experiments consisted in standard testing tubes of 10 ml (NS 12/21, 10 ml, Ø 15 mm), and for the spinning drop tensiometer measurements special capillary tubes FEC 622/400-HT were used (Figure 22).



Figure 22. Testing tubes for Phase Behavior experiments, and capillary tubes for Spinning Drop Tensiometer measurements.

The following solvents were used for cleaning purposes:

- n-Decane $\geq 95\%$ (A. ALDRICH)
- Acetone $\geq 99.9\%$ (ROTH)
- Toluene, 99.8% (SIGMA-ALDRICH)

The cleaning process consisted of a sequential dissolution of the oil in the recipients by flushing the oil with the chemicals previously listed. The sequence used consisted of n-Decane > Acetone > Toluene > Acetone > Distilled water.

For the capillary tubes used with the Spinning Drop Tensiometer device, an additional cleaning step was used. For it, the capillary tubes were treated with an ultrasonic bath (Figure 23) for at least 15 minutes.



Figure 23. Ultrasonic bath, BADELIN-Sonorex.

The daily laboratory materials used for the experimental preparation can be summarized as:

- Syringes of 1, 5 and 10 ml (BRAUN)
- Syringes needles of 1.36x38.1 mm, 0.8x120 mm BL/LB, and 0.6x30 mm BL/LB
- Microscope Slides (Thermo scientific)
- Latex gloves (ROTH)

Finally, during the project sample A was observed under microscopy image technique, the microscope used is a device from KEYENCE model VHS-600, which provides an enlargement up to 2000x (Figure 24).

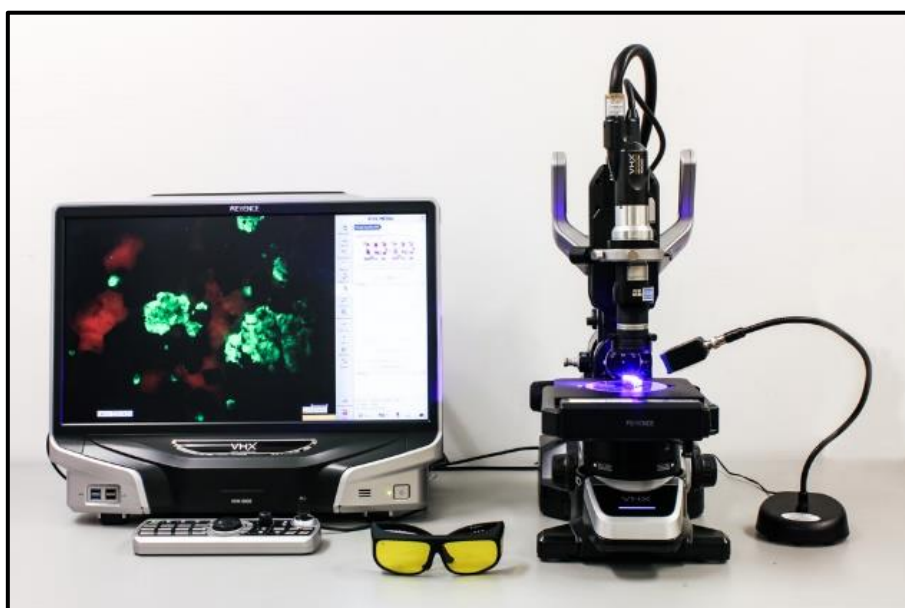


Figure 24. Digital microscope VHS-600, KEYENCE.

3.1 Spinning Drop Tensiometer Setup

The equipment used for the experiments reported in this work is the Spinning Drop Tensiometer STV-20 of DataPhysics Instruments GmbH.

The experimental setup consisted of mainly three systems:

- 1) Cooling/Heating system (Julabo CD-200F). Two Julabos were used, one to keep the temperature of the STV-20 motor low during the experiments, and a second Julabo was used to manipulate the temperature at the spinning drop chamber (Figure 25).
- 2) Measuring device (STV-20): The STV-20 DataPhysics measuring device consisted on 1) touch panel for operation without PC, 2) digital camera, 3) measuring chamber, and 4) motor (Figure 26).

3) PC control software (STV-20): From the software panel, a diverse number of parameters could be controlled during the measurement such as rotational speed, chamber inclination, and camera position, among others.

This work does not provide the description of the Spinning Drop Tensiometer usage, due to the previous work reported regarding this equipment usage. A detailed description of the system usage, equipment preparation, and available operation modes are provided in (Arnold, 2018).



Figure 25. Cooling/heating Julabo CD-200F

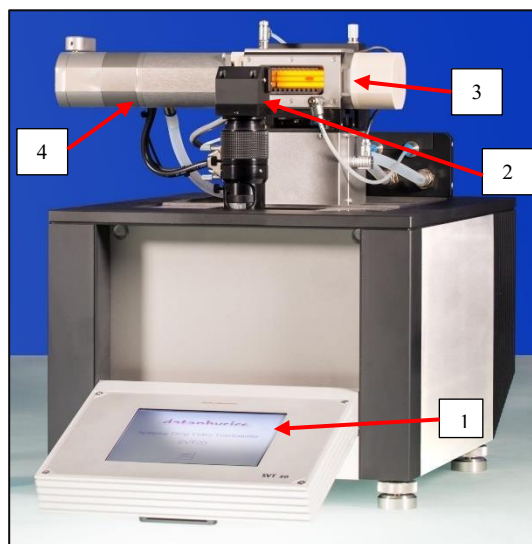


Figure 26. Dataphysics STV-20 components.

Chapter 4

Puchkirchen Field and Fluid Characteristics

In this chapter, the Puchkirchen field characteristics and fluid properties used in this research project will be presented. The sampling methodology will be reviewed, and the measures taken to separate the sample into the oil and water fractions.

Table 1 summarizes the Puchkirchen field and the well characteristics from which the fluids were retrieved:

Table 1. Field and well characteristics

| Field Characteristics | | |
|------------------------------|-----------|---------------------|
| Connate Water Salinity | 2.8 - 4.5 | g/l |
| T_{res} | 94 | °C |
| API | 33 | degree |
| Oil Viscosity, μ_o | 1 | cP at Res. Cond. |
| pH | 7.6 | |
| RF (current) | 15 | % |
| P_{res} (East) | 230 | bar |
| P_{res} (West) | 150 | bar |
| <i>Well A Depth</i> | 2543.5 | <i>m [MD]</i> |
| Well B Depth | 2599.5 | m [MD] |
| Distance between wells | 600 | m |

4.1 Well Sampling

Special attention into the sample retrieval was given; the target was to obtain representative samples, which implies that no additives must be present in the system at the sampling moment. Meanwhile, well A was producing additive-free oil and water, well B was being treated with corrosion inhibitor (bottom-hole injection). In order to reduce the additive fraction on the sample, the additive injection was stopped one week before the samples were retrieved.

The two wells were sampled at the wellhead, and the sampling procedure involved purging the superficial sampling valve from non-representative fluids before sampling the wells. Therefore, an initial volume of 5 liters of fluid was allowed to flow, before retrieving the oil and water from each well. Accordingly, to production data, different water fractions were expected in each well, where Well A produced a mixture containing a water cut of 24% and Well B 55%.

4.2 Fluid Separation

The starting point in each set of experiments that one can think will involve a blank test. The desired blank test in this thesis was to measure the current interfacial energy between pure oil and brine. Hence, measures to separate the water from the oil were taken.

It is broadly known that in order to separate the fluid phases with not much effort, one can set the samples at rest and let the gravitational field perform its own job. It is expected that due to buoyancy forces, both fluids will separate by density difference and the droplets after flocculation will coalesce. However, a tendency of the sampled fluids to stabilize emulsions into an emulsion type II (+) in the Winsor's Ratio was observed. The presence of stable emulsions made the separation time much longer or maybe almost infinite. The common practice for fluid separation is the use of demulsifiers or emulsion breakers.

Due to the initial target of the research was to apply alkali solutions to reduce the interfacial tension, the use of this additive was not an option for this project. Hence, if the emulsion breaker was used, a change in the interfacial energy will be induced. Then the measurements will no longer record the natural state of energy of the system, and the measurements cannot be used as a relative point versus the alkali performance. Then, separation methods that could affect the least the fluid composition nor interfacial energy were tested.

In the first instance, the separation by **temperature** in as much as 94°C (reservoir temperature) did not provide an actual separation of the fluid phases; then **centrifuge** was used as the next separation method to be tested.

4.2.1 Centrifuge

The method of artificially increasing the gravity field by centrifuging the samples A and B (A and B stand for the samples retrieved from Well A and B respectively) was tested. The target is to induce the water droplets to deposit, flocculate, and coalesce into bigger water droplets faster. A small amount of both samples (80 ml) were centrifuged at 2000 rpm for 130 minutes at room temperature, 23°C. Contrary to a water and oil phases separation, a highly viscous fraction deposited at the bottom of the recipient (Figure 27). The most noticeable feature that could be noted between the fluids A and B after centrifuging was the amount of the “heavy fraction” in the two samples. Being the heavy fraction of sample B greater than the one seen at sample A.

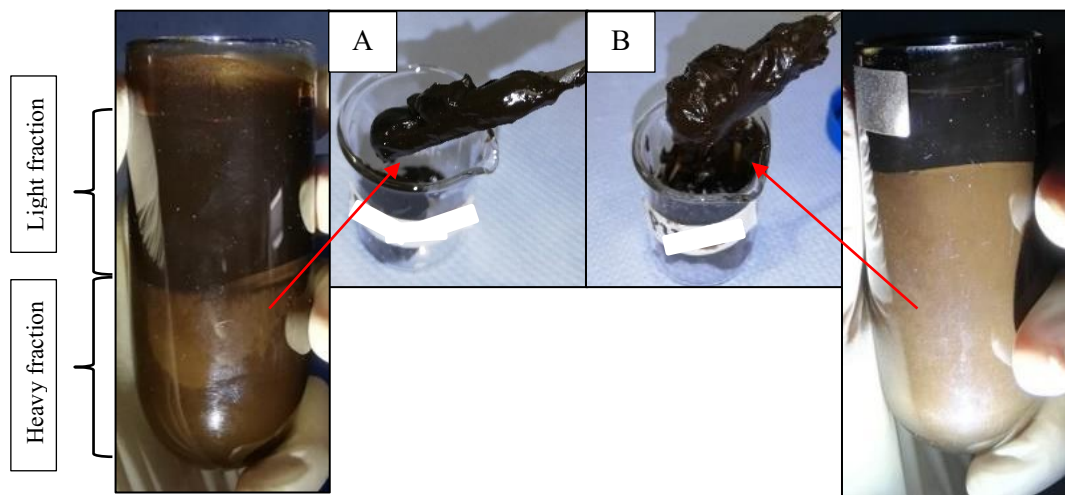


Figure 27. Samples A and B after centrifuging at 2000 rpm and 70 minutes @ 23°C. At the top left of each sample the separated emulsion fraction.

Later experiments showed that the heavy fraction was in fact **emulsions**. It turns out that the emulsions could not be broken by centrifuging. It seems that the emulsifying agent present in the system is so stable that it allowed the emulsions to settle down and flocculate along with other heavier components of the oil but avoiding their coalesce with the neighboring emulsions.

The outputs of the centrifuge experiments were not a clean oil for interfacial tension measurements for alkali application, neither water for titration experiments, but a light oil fraction or emulsion free fraction (upper fluid in the recipient), a heavy fraction (emulsions plus the heavy components of the oil), and the knowledge of emulsions being stable at high temperatures and centrifugal forces in as high as 4400 m/s^2 .

Interestingly, the sample with the lower emulsion fraction showed the lower viscosity as well. Then, in order to corroborate the water contained in the oil samples, the emulsion breaker was applied at 60°C (5000 ppm). After 48 hours at rest, the sample A expelled 24.4 % of water and

sample B 54.9 % of water (Figure 28), both results (± 0.1 ml) agreed with the reported water cuts coming from production data.



Figure 28. Water fraction in samples A (right) and B (left).

The output of the centrifugal experiment provided two fractions that could be used for the IFT experiments a “light fraction” or full¹ sample. Then in order to select a proper fraction for the spinning drop tensiometer experiments, it was decided to perform phase behavior tests on both full and the light fraction of samples.

4.3 Phase Behavior of Full and Light Fraction Samples

The hypothesis of the use of any of both samples for experiments can be addressed in the next lines:

- **Usage of Full Sample**

At this point, the Alkali potential was under evaluation. Then, it was desired to measure the effect of the generated surfactants on the IFT reduction. Then a system with a fraction of emulsified water may reduce the alkali effect on IFT reduction.

- **Usage of Light Fraction**

If the light fraction lost an essential fraction of heavy components while centrifuging, the IFT would be laying into non-realistic results. As the ASTM D-664-6a relates, an essential

¹ Full sample refers to the fluids as retrieved from surface with emulsified water contained in it.

fraction of the fatty acids is encountered in the heavy hydrocarbon molecules. Then the alkali reaction may be limited by the precipitation of these components while centrifuging.

Then, the reasoning that pushed the phase behavior experiments was: If we considered both samples as equally representative, then in principle, they should behave as equal.

The initial phase behavior experiments involved the use of the full sample A. In this experiment, the full sample A plus distilled water was used (Figure 29-1). Additionally, in order to test the salinity effect on the phase behavior, the second system of full sample A and 2.8 g/l NaCl brine² was used (Figure 29-2), the concentration and fluid volumes are resumed



Figure 29. Phase behavior of full sample after 48 hours at 60°C. 1) Oil plus distilled water, and 2) oil plus 2.8 g/l NaCl.

Table 2.

Table 2. Fluid volume and salinity concentration for phase behavior tests.

| Experiment | Salinity [g/l] | Oil [ml] | Brine [ml] | Temperature [°C] |
|------------|-------------------|-------------|---------------|---------------------|
| 1 | - | 5 | 5 | 60 |
| 2 | 2.8 | 5 | 5 | 60 |

² Later experiments showed the actual brine salinity of the brine was 4.5 g/l NaCl. The effect of salinity in the interfacial tension changes, by dynamic interfacial tension measurements, was found to be negligible.

The next experiments substituted the full sample A for light fraction A. Distilled water and 2.8 g/l NaCl were used as well. Figure 30 shows the results after the experiments.

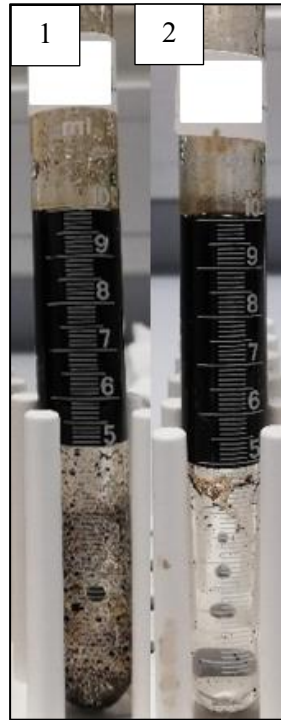


Figure 30. Phase behavior of light fraction sample after 48 hours at 60°C. 1) Oil plus distilled water, and 2) oil plus 2.8 g/l NaCl.

Both experiments of full and light fraction samples were performed at 60°C. The sequence in which the experiments were performed involved the pre-heating of the systems before agitation, followed by letting the samples at rest for 48 hours for stabilization.

The results from the experiment showed a clear phase behavior difference between both types of samples. Meanwhile, the final state of the systems containing light fraction resulted in a sharp interface water-oil, the full sample A contained natural surface-active material that emulsified the brine under turbulent conditions.

Figure 31 illustrates a possible explanation of the observed phenomena. It shows the fluid before and after the sample centrifuging. What is shown in Figure 31-A is the system prior to the centrifugal forces, where one can encounter emulsified water drops, solids, and asphaltenes in suspension. Whereas the right Figure 31-B shows the sample after centrifugal forces have been applied, where the heavy components contained in the oleic phase have deposited at the bottom of the recipient.

One can notice the green sections on the figures which are not only in suspension but coating the water droplets as well. This green fraction is hypothesized to be responsible for the water

emulsification in the system. It is represented as a colloid because it is available for any polar component that enters in contact with it.

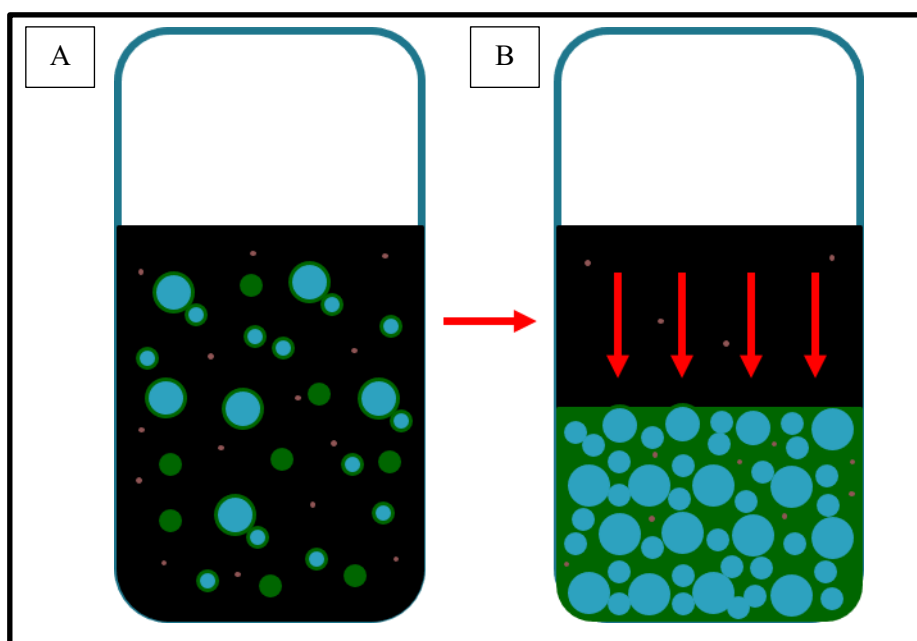


Figure 31. The before and after of centrifuging samples A and B

The risk of separating the carboxylic acids from the light fraction while centrifuging became prominent since these acids are mainly found in the heavy fractions of the oil. The output of these experiments is the decision of discarding the light fraction for further experiments and continue the work with full samples.

Then as reviewed in **Chapter 2** in the Natural Surface-Active Agents section, a possible explanation for the emulsions in the samples could be provided by taking a closer look into the samples.

4.4 Emulsion Characterization

As mentioned, the two theories of emulsion stabilization material that often appears in the oil industry is ruled by mainly finely divided particles and asphaltic molecules. In order to find out the responsible surface-active agent that causes the emulsion stabilization in the fluids, sample A was investigated by microscopy. Lake (2006) shows how one can perceive emulsion stabilization by finely divided particles. Their presence is denoted by a dispersed finely laminar material in the oleic phase. The purpose of the microscopy investigation was then to perceive indices of the existence of fine particles in the system.

The digital microscope used (VHX-600) allowed us to characterize emulsions in a range size of 1-250 μm . The emulsions in the system were classified by the dispersed phase, being emulsions type II (+) in the Winsor classification (Figure 32). From the microscopy photograph

in Figure 32 can be seen how emulsions cover regions of intensive emulsion presence; meanwhile, other regions appear to be cleaner. The brownish regions in the micrograph photos are the continuous oil phase, and the white and black dispersed spheres are the emulsified water. The water emulsions in the photograph appear like dark regions in the oil; this effect is perceived because as the light passes through the emulsified water diffracts changing its trajectory to other directions around the water spheres and light beams cannot reach the microscope lens. The emulsions in sample A flocculate to form emulsion clusters, but with the particularity of avoiding coalescence into bigger droplets.

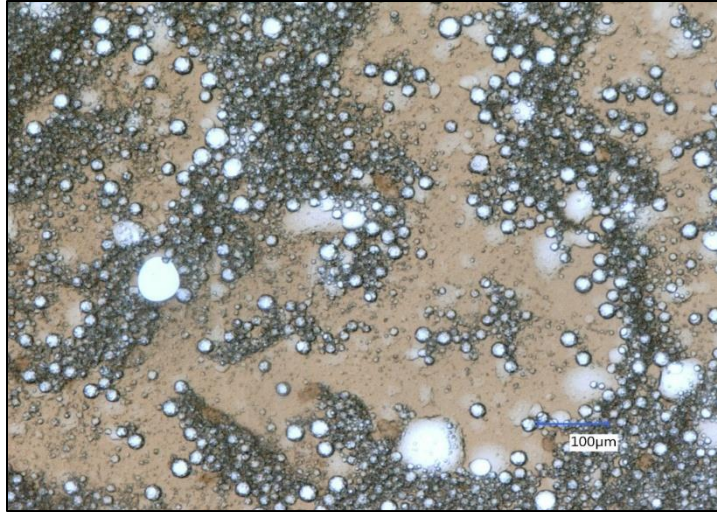


Figure 32. Micrography of water into oil emulsions contained in sample

A.

At first glance and based on the microscopy showed in Figure 33, the emulsion size was found to be ranging from 1 μm up to 20 μm. Under the current laboratory capabilities, it is not possible to know whether or not smaller emulsions than 1 μm exists in the system.

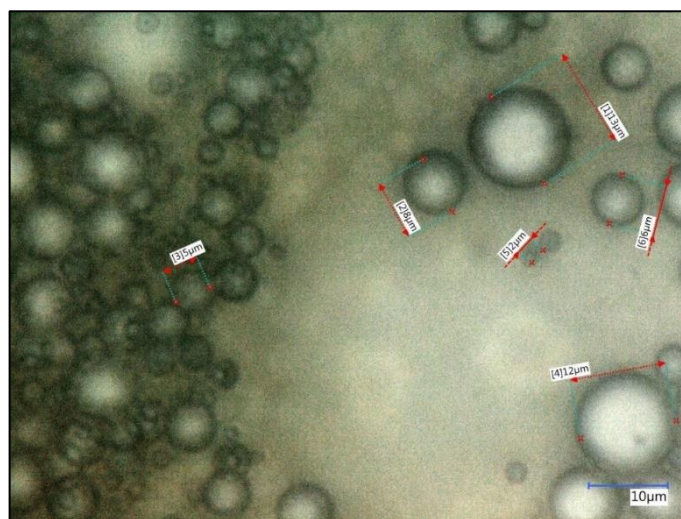


Figure 33. Sample A emulsions. Emulsion size varying from 1 μm up to 13 μm.

Then, in order to further characterize the emulsions, image analysis was performed on the microscopy images from sample A (*Figure 34*). The output of the analysis is the emulsion size distribution in a normal distribution function (*Figure 35*). From which one can denote that the emulsions are mainly laying into the tight emulsions range, as previously shown in *Figure 16*. This is characterization also agrees with the previous experiments performed, in which emulsions exposed themselves as highly stable to the reservoir temperature (94°C) and centrifugal forces.

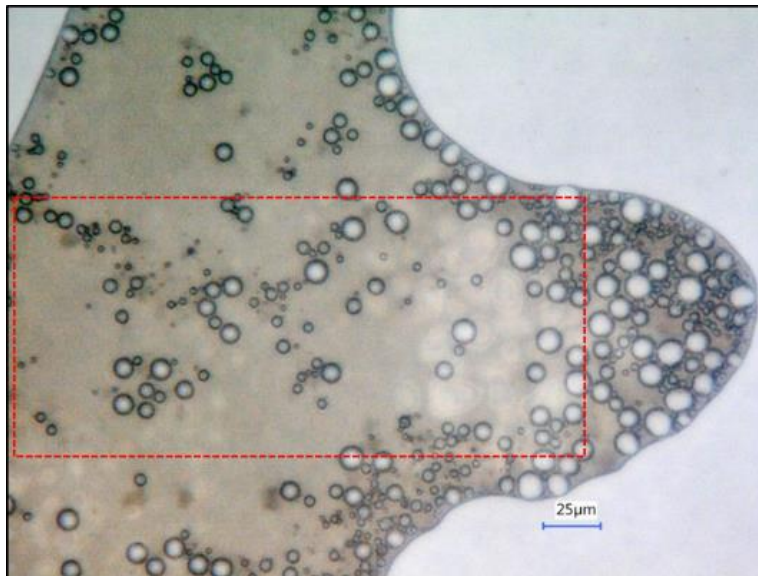


Figure 34. Emulsion microscopy from sample A used for emulsion size distribution. Section used denoted by the red dashed lines.

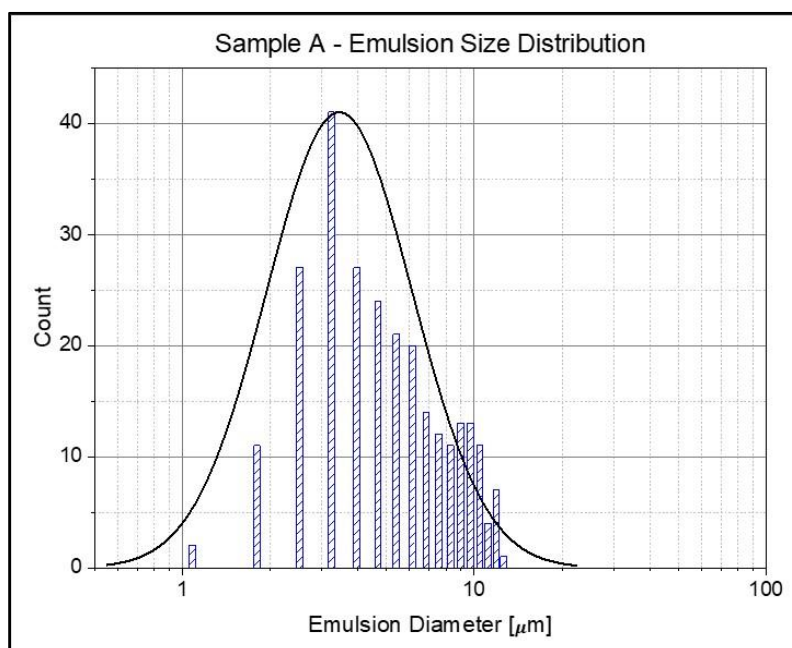


Figure 35. The emulsion size distribution of sample A showing a normal distribution in the range of tight emulsions.

Chapter 5

Experiments

This chapter is dedicated to the experimental results recorded while working with the full sample A and brines containing different salinity concentrations and emulsion breaker. **In this Chapter, the full sample A is referred to as sample A.** Moreover, the experiments concerning the Alkali application are omitted. As previously mentioned, the performance of Alkali solutions on interfacial tension reduction was found to be limited, but its interaction with the reservoir rock was not covered during this research. During this chapter, the results from the phase behavior and Spinning Drop Tensiometer will be presented. The experiments involved blank tests, variations in salinity, and emulsion breaker concentrations.

5.1 Phase Behavior

The first set of phase behavior experiments were dedicated to observing how the system will behave under different conditions of salinity, temperature, and emulsion breaker concentrations. For it, blank experiments were performed. These experiments involved 5 ml of oleic phase and 5 ml of water/brines. Then, the emulsion breaker was used in order to perceive any significant changes in the phase behavior.

5.1.1 Salinity Effect

The range of salinities used in the experiments can be cataloged as low salinity. This due to the produced formation water salinity reported at the Field. The produced salinity ranges within the low margin of 2500 ppm up to 4500 ppm over time. The initial experiment involved distilled water (Figure 36-A), followed by a brine containing 2.8 *g/l NaCl* (within the salinity reported of the field) (Figure 36-B), and finally a salinity of 12 *g/l NaCl* (Figure 36-C).

The results from these experiments showed emulsifying tendencies and small variations of brine volumes. The two extremes of no salinity and high salinity (Figure 36 A and C), did not provide a significant effect that could be perceived and used as a screening parameter for interfacial tension. Both systems developed 3 phases, a lighter upper phase, an emulsion phase (middle), and a small fraction of water at the bottom of the recipient. These emulsions were

classified as to be water in oil emulsions, Type III in the Winsor's ratio. On Figure 36-B where the salinity concentration 2800 ppm was used, a greater fraction of the emulsified water was expelled from the system. However, the result of these experiments was not practical and could not be used as a clear screening criterion.

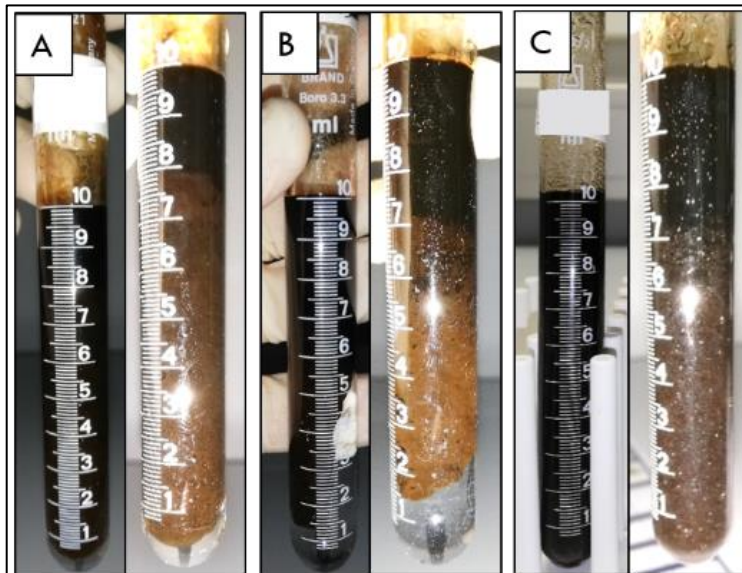


Figure 36. Phase behavior - Salinity effect (a) zero, B) 2800 and c) 12000 ppm salinity) on the phases generated in the system.

5.1.2 Temperature Effect

The next step was to observe the effect of a range of temperatures on the system behavior, starting by the ambient temperature of 24°C (Figure 37-A), 60°C (Figure 37-B), and 94°C (Figure 37-C). For it, the brine that mimics the salinity of the field, 2.8 g/l NaCl, was kept constant during these tests. These experiments were performed using sample A and all experiments involved 5 ml of oil and 5 ml of brine.

Figure 37 shows the temperature effect on the phase behavior, as the temperature is increased, the greater the water fraction being expelled from the emulsion phase can be achieved. These experiments agree with the emulsion destabilization mechanisms reported by Larry Lake, 2006, in which by temperature the viscosity of the mixture decreases allowing the emulsions to settle faster and flocculate, then due to thermal expansion the emulsified water increases its volume making the coating film of surface-active material thinner.

The fluid behavior showed in Figure 37 is interesting, especially the one showed in Figure 37-C, in which emulsions on the system can be perceived even by the naked eye. Those emulsions are highly unstable to disturbances such as low mixing energies. The output of these experiments is emulsions that are mechanically unstable at 94°C and atmospheric pressure.

However, a clear screening criterion could not be used from the changes in salinity nor temperature.

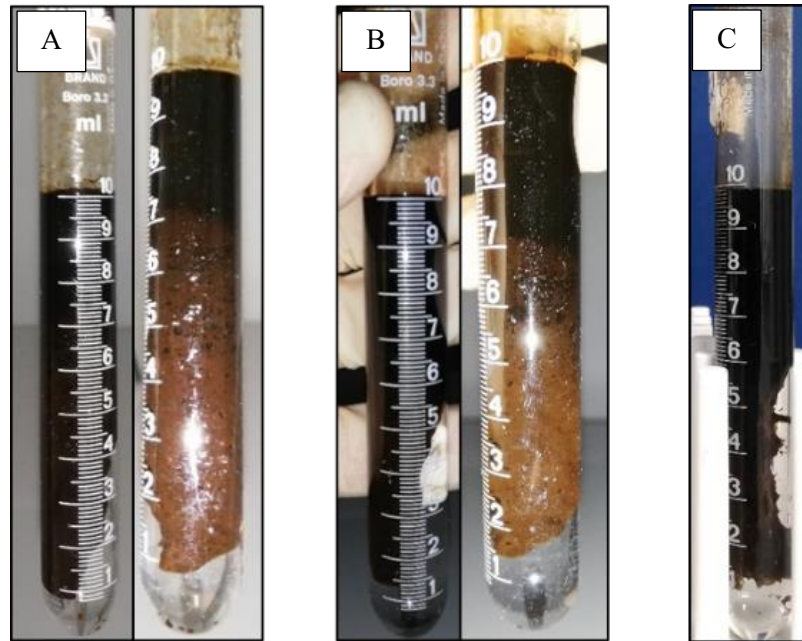


Figure 37. Temperature effect on phase behavior, A) 24°C B) 60°C, and C) 94°C. It is shown next to figures A and B an emulsion gradient in the samples. Whereas at 94 °C a gradient could not be perceived but a sharp envelope separating oil and the emulsions.

5.1.3 EMB – Ambient Temperature Effect

The next step included a range of emulsion breaker A concentration, targeting in the first instance to observe the demulsifier action under ambient conditions, 24°C. Each of the four systems consisted of 5 ml brine containing 4.5 g/l NaCl and 5 ml of oleic phase. The emulsion breaker concentration range used was 50, 76, 131, 190 ppm. Figure 38 shows the phase behavior experiment after 48 hours at rest. The emulsions in the systems were partially broken, leaving a translucent lower fraction, but no sharp interfaces were generated.



Figure 38. Phase behavior of systems containing emulsion breaker at different concentrations (50, 76, 131, 190 ppm from left to right respectively) at ambient temperature.

5.1.4 EMB – Reservoir Temperature Effect

Following this course, the additional experiments aimed to enhance the surfactant effect by reducing the action time of the demulsifier. For it an increase of the kinetic energy of the surfactant was desired; hence, the temperature was raised up to the reservoir temperature of 94°C.

For the experiments performed at reservoir temperature, it was decided to wide up the range of emulsion breaker concentration to both extremes, lower and higher concentrations. The hypothesis for this experimental set up consisted mainly in to be able to observe a kind of expelled brine gradient. Whereat low emulsion breaker concentration would provide a low water fraction liberated, and high emulsion breaker concentration may be translated into an increase of free water in the system. Then, a minimum surfactant concentration may be found.

Additionally, titration experiments to the reservoir brine were performed to corroborate the water salinity on the field. From which the reservoir salinity was found to have a concentration of 4500 ppm of NaCl. From this point and on, the salinity of 4500 ppm NaCl substituted the previously used of 2800 ppm NaCl.

The setup used in the experiments is summarized in the following table:

Table 3. Experimental setup of phase behavior using low emulsion breaker A concentration.

| Experiment # | Demulsifier ppm | Brine Salinity ppm | Brine Vol. ml | Sample A Vol. ml |
|---------------------|------------------------|---------------------------|----------------------|-------------------------|
| 1 | 18 | 4500 | 5 | 5 |
| 2 | 37 | 4500 | 5 | 5 |
| 3 | 50 | 4500 | 5 | 5 |
| 4 | 74 | 4500 | 5 | 5 |
| 5 | 150 | 4500 | 5 | 5 |
| 6 | 190 | 4500 | 5 | 5 |
| 7 | 232 | 4500 | 5 | 5 |

Even though the systems expelled the emulsified water fraction in several minutes, the systems were set to rest for 48 hours to perceive any posterior changes. After this settling time, no further changes were perceived — the experiments where pre-heated up to 94 °C before they were mixed.

Figure 39 shows the seven systems after 48 hours, from lower to higher concentrations, left to right, respectively. Contrary to the expected water fraction gradient, all the systems expelled similar water fractions of the emulsified water in the oil, about $25\% \pm 5$ (corroborated individually by image analysis). The expelled water fraction agrees with the reported water cut of the well.



Figure 39. Emulsion breaker concentration variation after 48 hours at reservoir temperature, 94 °C. The red line defines the envelop at which the water-oil interface was allocated at the beginning of the experiment.

5.2 Interfacial Tension Measurements

As the phase behavior experiments could not be used effectively as a screening tool for the different solutions, the screening criterion was applied by dynamic interfacial tension measurements. In order to observe the natural interfacial energy of the system, experiments involving distilled and **2800 ppm NaCl** solutions were performed. These tests will serve then as a relative point for comparison to the solutions, including emulsion breaker. In this section, blank test experiments are presented, followed by the brine solutions containing emulsion breaker at different concentrations will be shown.

5.2.1 IFT – Distilled Water

The experimental setup involved the use of **sample A** and distilled water. The experiment was carried on at **6000 rpm**, and due to technical limitations, the experiments were performed over a range of temperature starting **20 °C to 50 °C**. During the measurement the system was allowed to achieve stabilization at 20°C which could be perceived as a plateau, from that point the temperature was progressively raised at 10°C until 50°C. On each temperature step, a stabilizing time was provided as well. During this experiment, the IFT remained quite constant and without evident IFT changes over the ranges of temperatures, where the average IFT value of **26.68 mN/m** can be reported. Additionally, the drop shape remained constant over time, and a normal increase in drop volume when the temperature was raised was recorded.

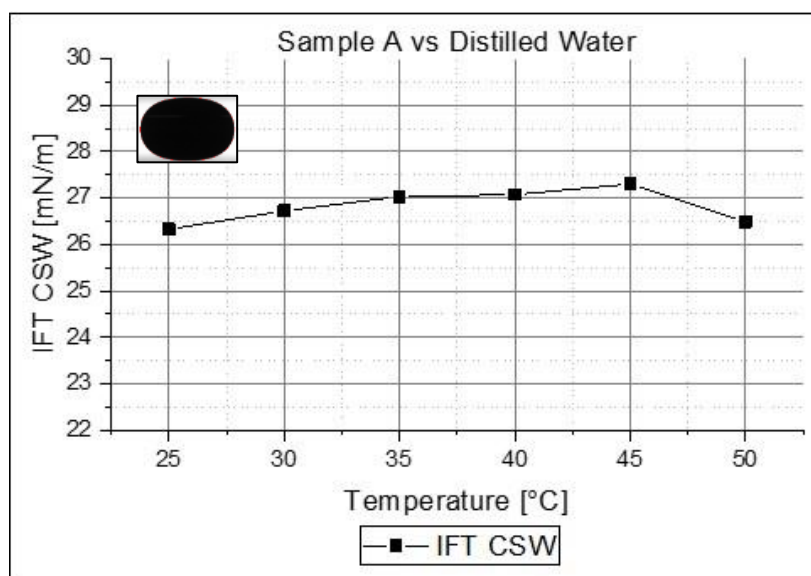


Figure 40. Dynamic interfacial tension measurement of Sample "A" vs distilled water, at 6000 rpm.

5.2.2 IFT – Reservoir Salinity

The next experiment target to mimic the salinity of the reservoir brine, as the initially reported of **2.8 g/l NaCl (2800 ppm)**. The process that this experiment followed was the same as the one performed for distilled water measurements. The interfacial tension over the range of temperatures from **20°C to 50°C**, and at a rotational speed of **6000 rpm** remained constant, and no sudden changes were perceived. The average **IFT** value over the temporal domain of **27.64 mN/m** is reported, being the last the IFT value the comparison point for the EMB action. Finally, the droplet morphology remained constant, and volume continued its normal expansion as the temperature was raised from low to high temperature.

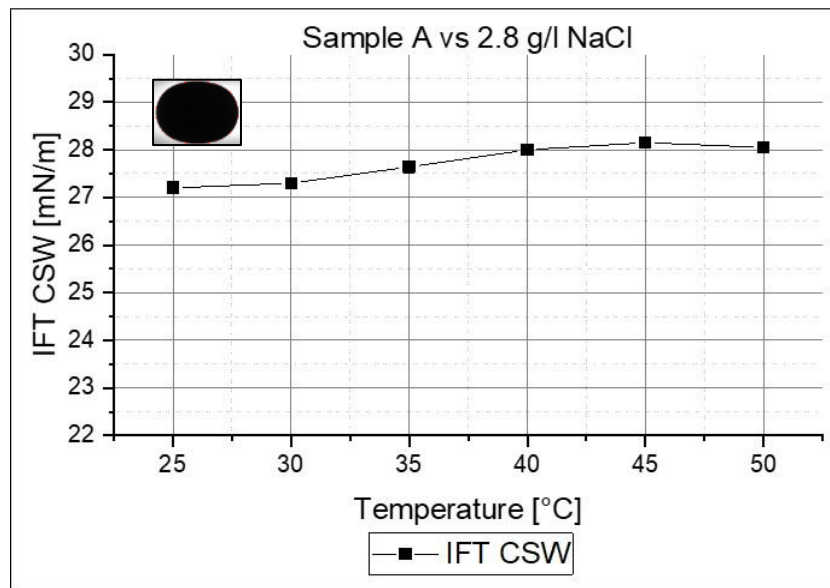


Figure 41. Dynamic interfacial tension measurement of Sample "A" vs 2.8 g/l NaCl, at 5500 rpm.

5.2.3 IFT – Emulsion Breaker

For these set of experiments, the brine salinity was changed to **4.5 g/l NaCl** due to titration experiments showed the actual formation water salinity. The angular velocity was kept at **3000 rpm** over the duration of all measurements. Moreover, the Spinning Drop Tensiometer setup was upgraded to be able to reach higher temperatures; then the temperature range was changed from 20 – 50 °C to **50 – 90 °C**. Being 50°C the starting point, from which the temperature was gradually incremented in steps of 10°C until 90°C was reached. Due to safety reasons, while working at high temperatures, the measuring time at 90°C was set as to be 90 minutes.

During the experiments with demulsifier, **the only variable** was the **EMB concentration**, being 18 ppm, 74 ppm, and 150 ppm of EMB. All other parameters remained constant; such as rotational speed, range of temperature, and duration time.

The hypothesis for these experiments was in principle to lower the interfacial tension of the fluids and to break the emulsions in the system simultaneously. If so, the initial interfacial tension of **27.64 mN/m** could be lower up to a certain degree, and the water demulsification may be perceived by an apparent reduction of the oil drop volume. Being caused the volume reduction by a mass transfer from the droplet to the continuous brine phase. Hence, the main parameters observed during the experiments were the interfacial tension magnitude and drop volume changes.

5.2.3.1 IFT – 18 ppm EMB

The initial experiments were performed using the lower EMB concentration because it showed similar results than the ones perceived at higher amounts of demulsifier (regarding the demulsification of the water fraction on the oleic phase). Being then the concentration of 18 ppm EMB the first brine to be investigated under the dynamic interfacial tension method.

The duration time of experiments showed on Figure 42 is about 4.7 hours long, as mentioned the rotational speed remained at **3000 rpm** and the fluids consisted in **sample A** in a brine containing **4500 ppm NaCl** and **18 ppm demulsifier**. The results showed an IFT reduction from slight to moderate, with a tendency of stabilization of the interfacial energy within the margin of 20 mN/m (± 5).

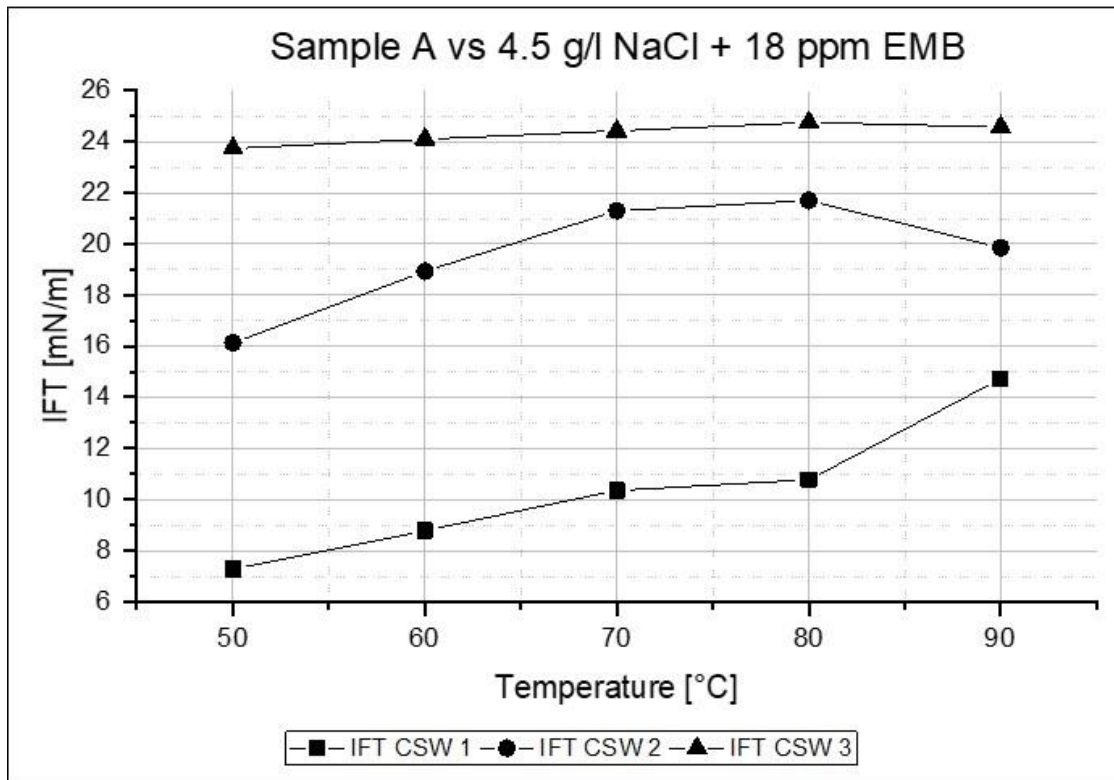


Figure 42. Interfacial tension measurements with solutions containing Sample A vs 4.5 g/l NaCl + 18 ppm EMB.

The same set of experiments is presented from the droplet volume change over time perspective (Figure 43), in which one can perceive almost constant droplet volumes regardless of the temperature increment.

Whereas in phase behavior experiments, the use of 18 ppm EMB appeared to have similar performance as the higher used concentrations (regarding emulsion breaking performance), on dynamic IFT measurements the IFT reduction was not optimum. Apparently, the effect of the demulsifier was limited by the small concentration.

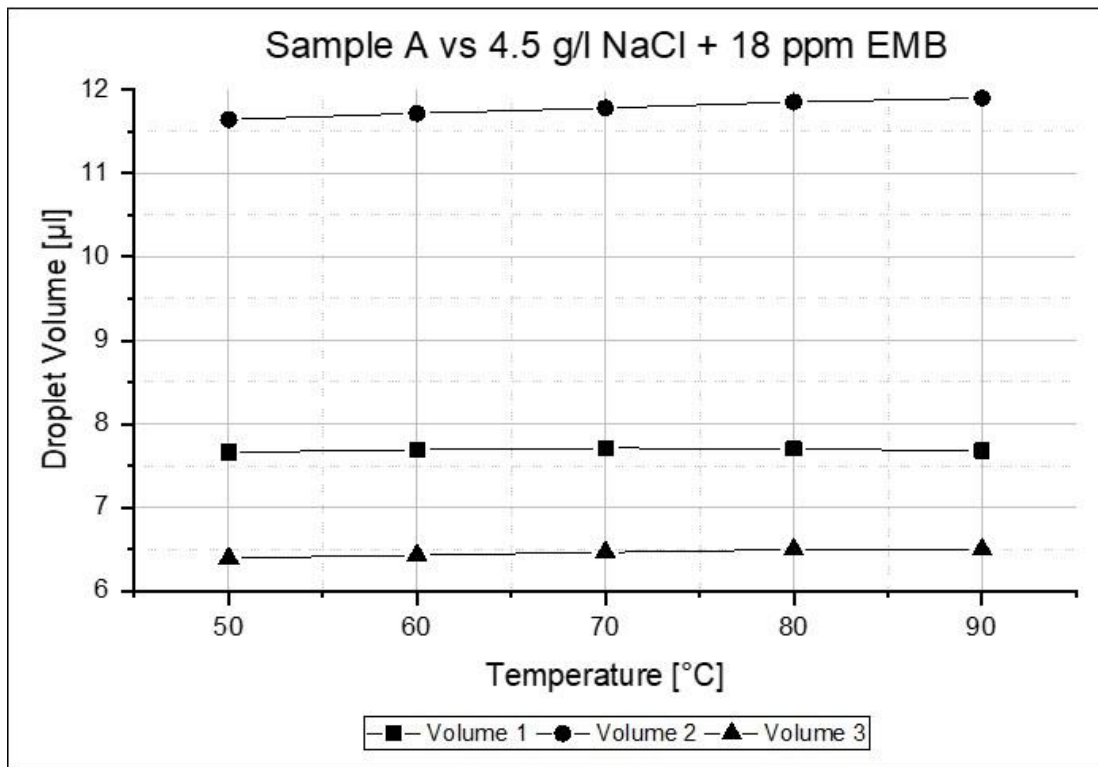


Figure 43. Droplet volume changes with solutions containing Sample A vs 4.5 g/l NaCl + 18 ppm EMB.

Experiments at **low demulsifier concentration** induced an **elliptical droplet shape** elongated in the “y” axis. The theorized reason for the droplet deformation is described in the following discussion section. The conclusion of this experiment was found to be limited regarding the IFT reduction and the demulsification of the water contained in the system.

5.2.3.2 IFT – 74 ppm EMB

The following experiments involved the use of a brine containing **4500 ppm NaCl**, **150 ppm** of **EMB** and **Sample A** for the experiments. The experimental sequence was the same as the one applied for the experiments involving 18 ppm of demulsifier. The starting temperature was 50 °C from which the temperature was increased in steps of 10 °C until a temperature of 90 and the angular velocity was kept as **3000 rpm**.

In this section, the interfacial tension and drop volumes are presented in Figure 44 and Figure 45, respectively. The output of the experiments includes interfacial tension reduction and drop volume reduction as the temperature increases. In the IFT measurements, the magnitude of the interfacial tension remained lower than the one observed with 18 ppm of EMB. However, the IFT measurements showed in Figure 44 varies in magnitude from low to moderate interfacial tension.

The droplet volume during the experiments showed an apparent contraction, regardless of the increase in temperature, which should provide a system expansion.

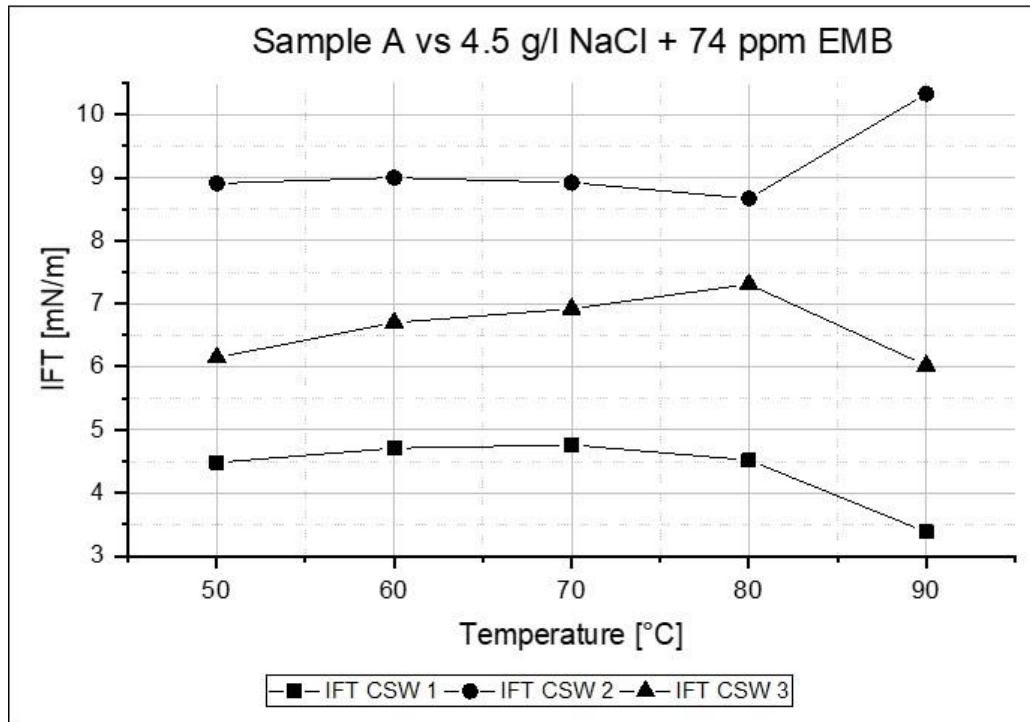


Figure 44. Interfacial tension measurements with solutions containing Sample A vs 4.5 g/l NaCl + 74 ppm EMB.

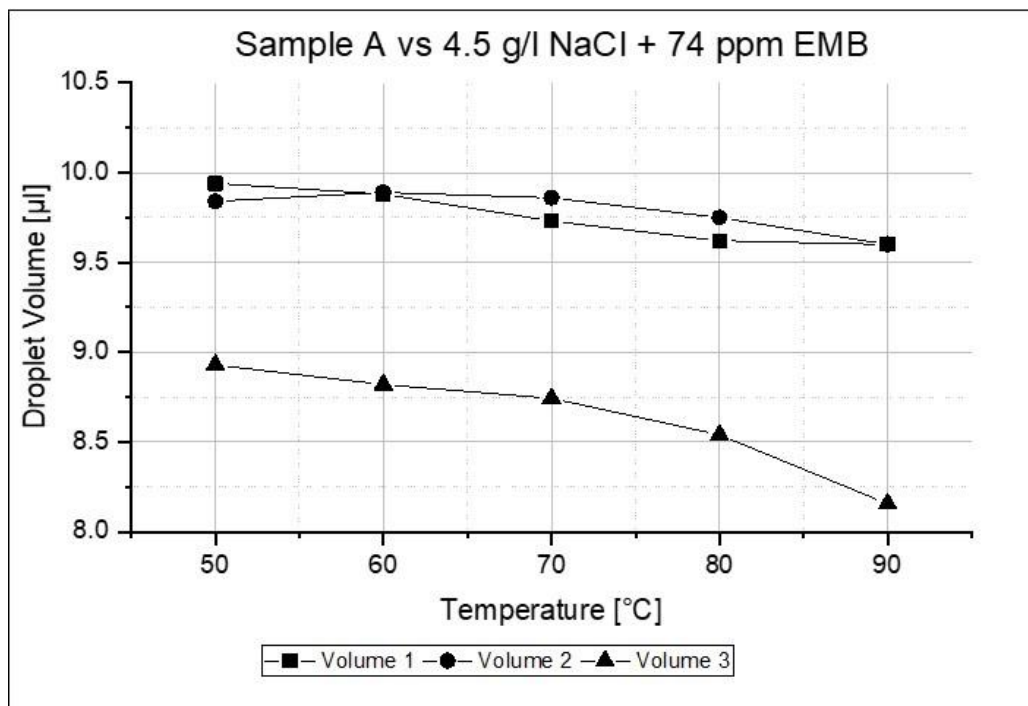


Figure 45. Droplet volume changes with solutions containing Sample A vs 4.5 g/l NaCl + 74 ppm EMB.

During some of the experiments, a balloon-shaped droplet appeared, its theorized reason for occurrence is described in the discussion section. Finally, to test if a further IFT reduction was possible, a brine containing 4500 ppm NaCl and 150 ppm of EMB was used.

5.2.3.3 IFT – 150 ppm EMB

The next set of experiments followed the same experimental procedure regarding stabilization time at the initial and final temperature. The temperature steps, angular velocity, and brine salinity remained as the ones used in previous experiments. Each experiments duration time was about 4.77 hours.

Figure 46 shows the interfacial tension measurements and temperature, where one can perceive an evident IFT reduction, relative to the recorded natural interfacial energy of **27 mN/m**. Notice that each temperature increment corresponds to an increase of interfacial tension of the system as well, but with the particularity of a sudden drop of IFT above the temperature of 80°C.

The other perspective of the same experiments consists of the droplet volume and temperature. The tests are displayed in Figure 47. With this perspective, one can notice the droplet volume changes as the temperature increased. Around 70°C up to 80°C, the droplet stops its expansion, and from that point and on, the droplet contracts as the temperature rises again. The final interfacial tension of experiment #2 was not recorded, due to the duration of the working time at 90°C, which did not allow stabilization.

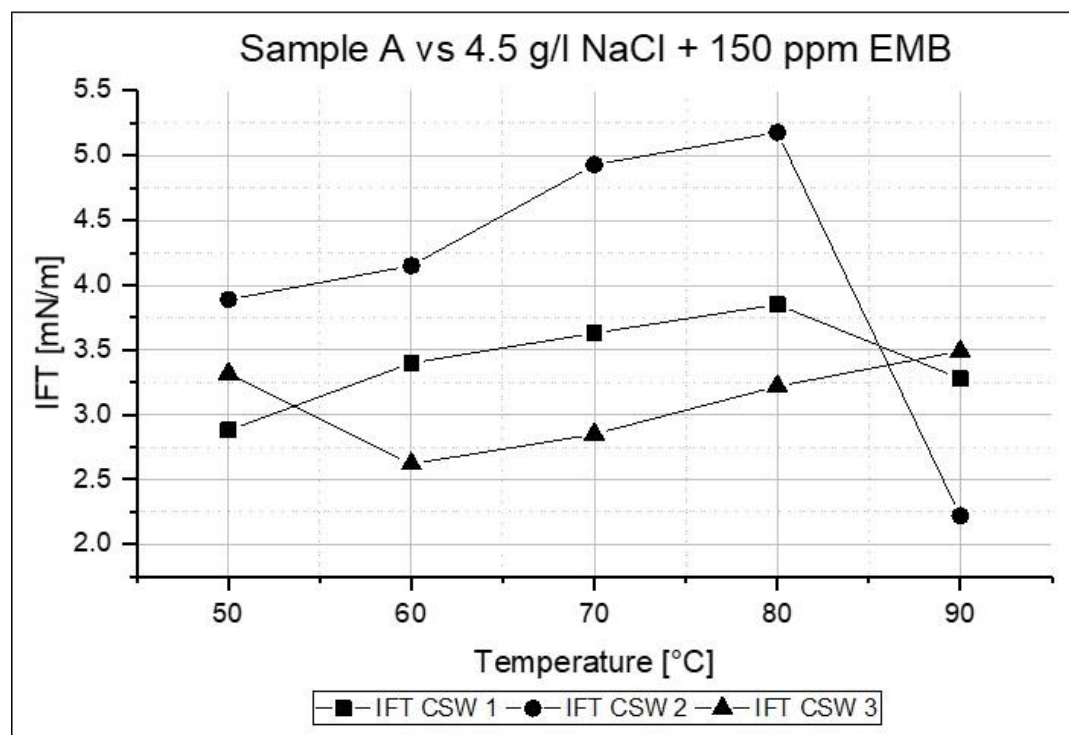


Figure 46. Interfacial tension measurements with solutions containing Sample A vs 4.5 g/l NaCl + 150 ppm EMB.

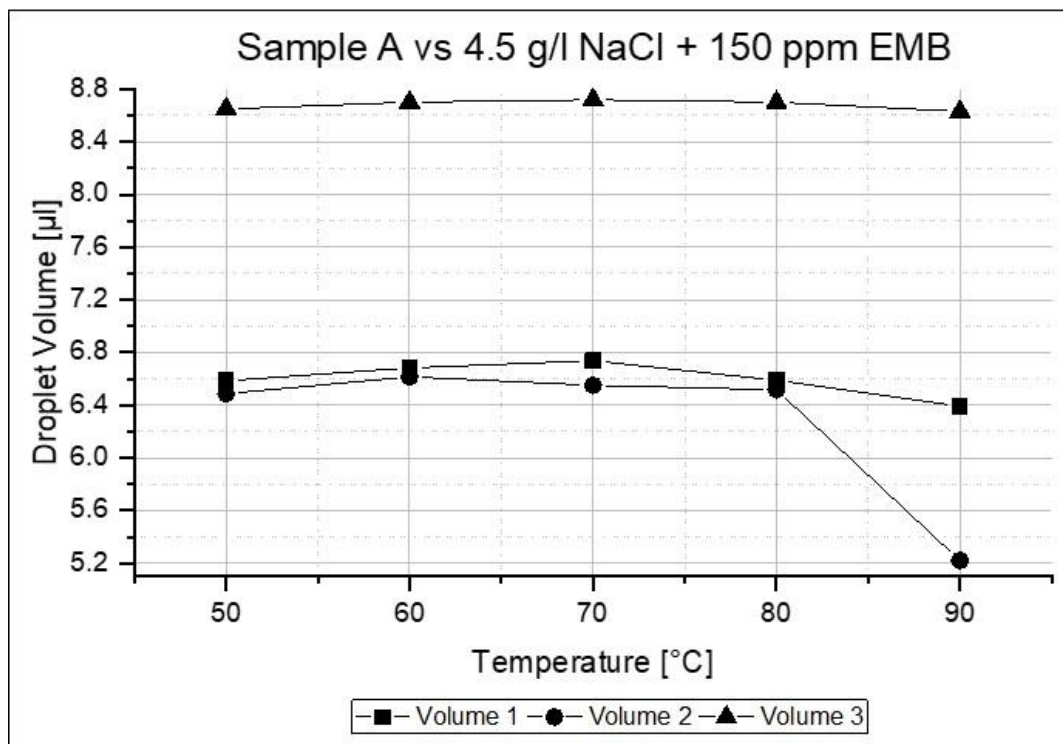


Figure 47. Droplet volume changes with solutions containing Sample A vs 4.5 g/l NaCl + 150 ppm EMB.

During the experiments at an early time, a drop stabilization occurred which is denoted by a gradual increase of the interfacial energy until a plateau is reached. During this period, sudden changes in the droplet topology were recorded as well. The description of these observed effects and the theorized explanations are provided in the next section.

5.2.3.4 IFT Comparison

Finally, a resume of the interfacial tension measurements is presented at the three different emulsion breaker concentrations and at constant temperature (Figure 48). Each plot shows the interfacial tension at 50, 60, 70, 80, and 90 °C, respectively. As one can perceive, as the emulsion breaker concentration is increased, not only the interfacial tension reduced but also the variation of the IFT.

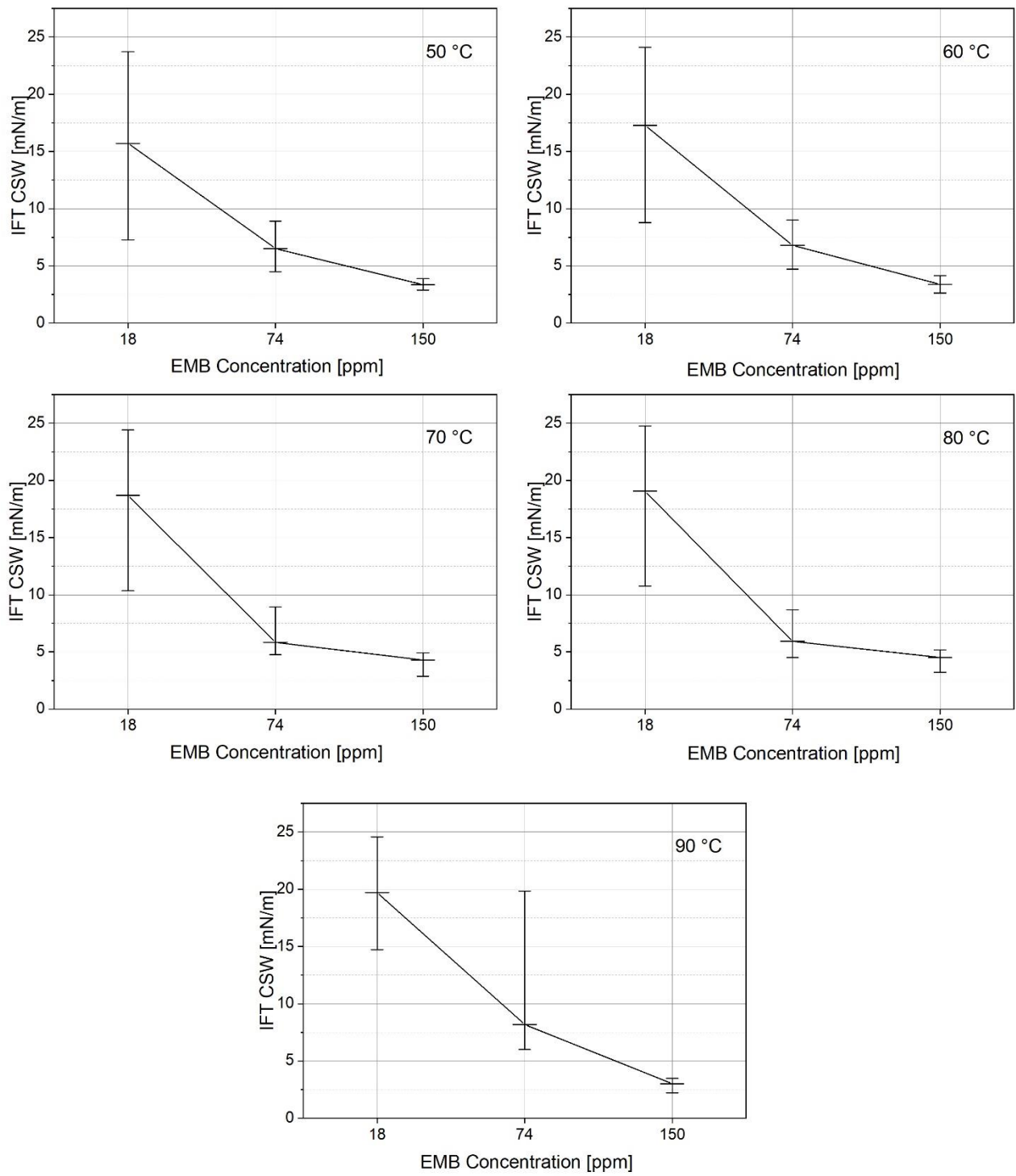


Figure 48. Interfacial tension measurements at constant temperature for different EMB concentrations.

5.3 Discussion

During the experiments performed with emulsion breaker solutions, interesting phenomena could be observed. Two main aspects of the experiments became evident:

- The apparent activation energy of the system related to the temperature at which the demulsifier increased its action. It was denoted by either the absence of a droplet volume expansion (constant volume over the range of temperature) as the temperature increased or by the reduction of the drop volume as the temperature increased.
- Droplet morphology deformation into irregular shapes: At low emulsion breaker concentrations (18 ppm), an ellipsoidal oleic drop could form (Figure 49-A), and at higher concentrations (74-150 ppm) a kind of ballooning effect developed, in which the shape is more than a semicircle on one side and a parabola at the other extreme (Figure 49-B).

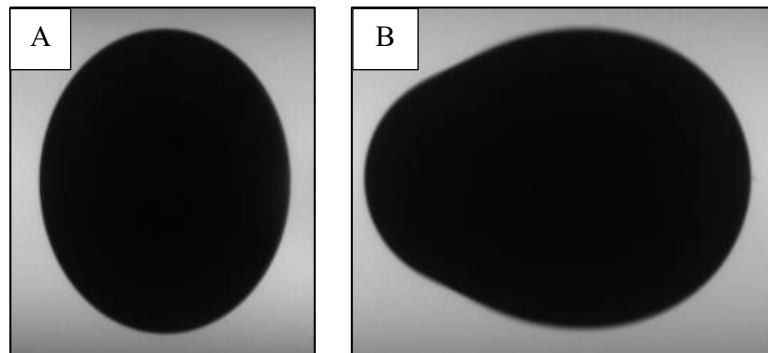


Figure 49. Oleic drop morphology variation while interacting at low and higher emulsion breaker concentrations in combination with high temperatures.

5.3.1 Ellipsoidal Deformation

Under the low concentration of emulsion breaker, a drop deformation in the “y” axis occurred, denoted by an ellipsoidal shape which remained over the range of temperatures. A possible explanation for the ellipsoidal deformation may be attributed to the reduced amount of emulsion breaker in the solution, which was not able to efficiently break all emulsion in the system. Additionally, the dispersed emulsions in the oleic phase, due to centrifugal forces allocate themselves by density difference at the interface of the droplet, generating a pulling effect towards the normal force axis of the centrifugal acceleration. A good example of the ellipsoidal deformation and the activation energy can be seen in Figure 50, where a system consisting of sample A and a brine containing 4500 ppm NaCl and 18 ppm EMB. In the following example, the ellipsoidal deformation remained during the whole experiment, and the interfacial tension in the experiment remained at an average value of **24.23 mN/m**.

Notice how in the range of temperatures from 50 to 80°C the volume change corresponds to normal expansion of the system, whereas above 80°C the volume expands slightly until 90°C where a smooth and constant reduction of both IFT and volume is recorded.

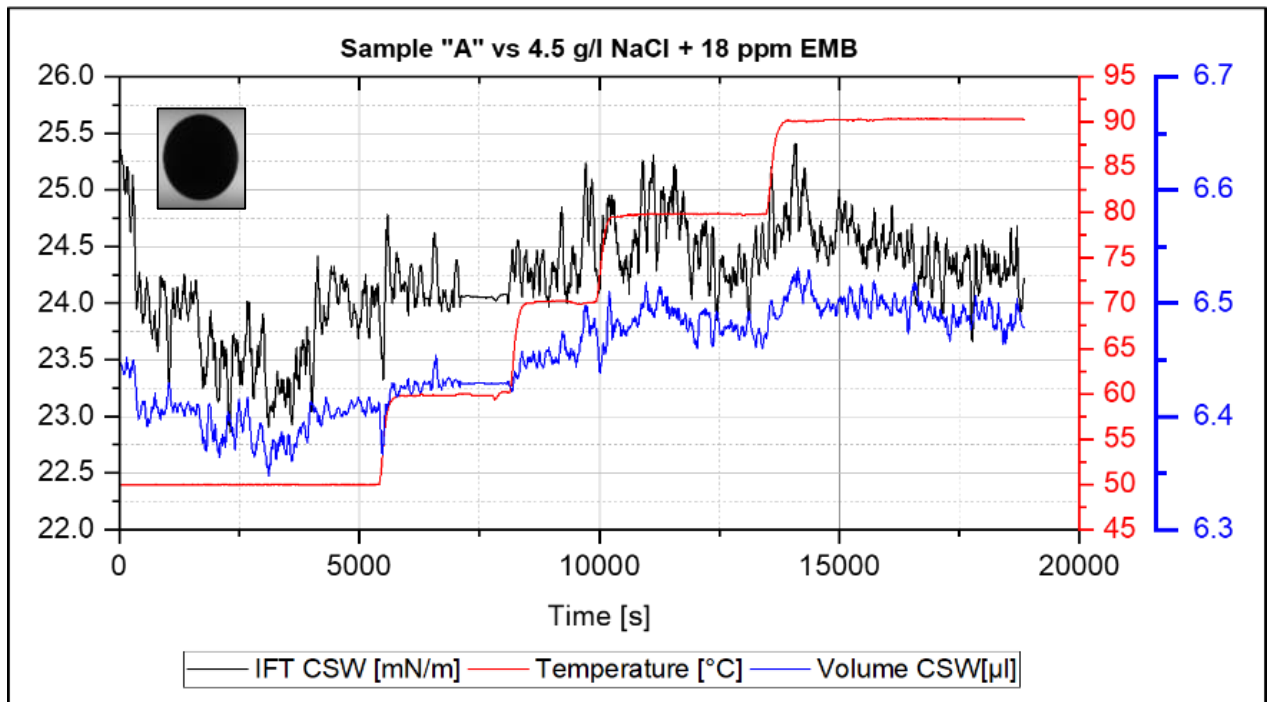


Figure 50. Interfacial tension measurement of Sample A vs 4.8 g/l NaCl and 18 ppm EMB, at 3000 rpm.

As literature relates, this effect may be a result of a combination of mechanisms acting to destabilize the emulsion drop; such as an enhancement of the molecular diffusion of the emulsion breaker in the system by an increase of the kinetic energy, and the reduction of the monolayer of surface-active material coating the drop by expansion of the material due to the increase of temperature. Since surfactants allow a system to generate new surface area with less energy (work), the area that could be generated due to the axial pull force of the emulsions is situated in the “y” axis (Figure 51).

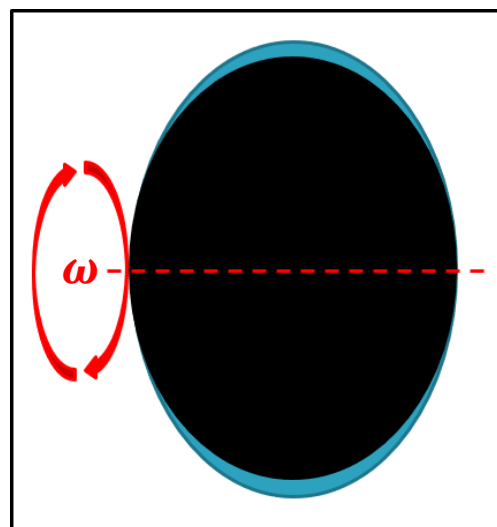


Figure 51. Ellipsoidal deformation of the droplet along the “Y” axis under low emulsion breaker concentrations.

5.3.2 Ballooning Deformation

For this explanation, the experiment containing 4500 ppm NaCl and 150 ppm EMB will be used. The angular velocity was kept to 3000 rpm during the measurement. As contrary to the previous experiments, in which as the temperature incremented it corresponded to volume expansion, the volume remained almost constant in the range from 50 to 80°C (Figure 52). The lowest interfacial tension recorded was **2 mN/m**. One will notice that the system did not achieve equilibrium, and it is due to technical reasons for the operation time of the equipment at high temperatures. Additionally, at early times as the droplet stabilized, changes in the droplet topology could be perceived. The drop initially had regular shape but at 1,200 seconds started to develop a balloon shape, in which one could encounter mainly emulsions coating the drop in the semicircular fraction of the shape, and an oleic fraction in the parabolic section. The increased amount of surfactant was able to fill any new area that could be generated allowing the sidewise expansion, which at the same time was being limited by the emulsion effect in the circular section of the drop. As the demulsifier breaks the emulsions causing the deformation

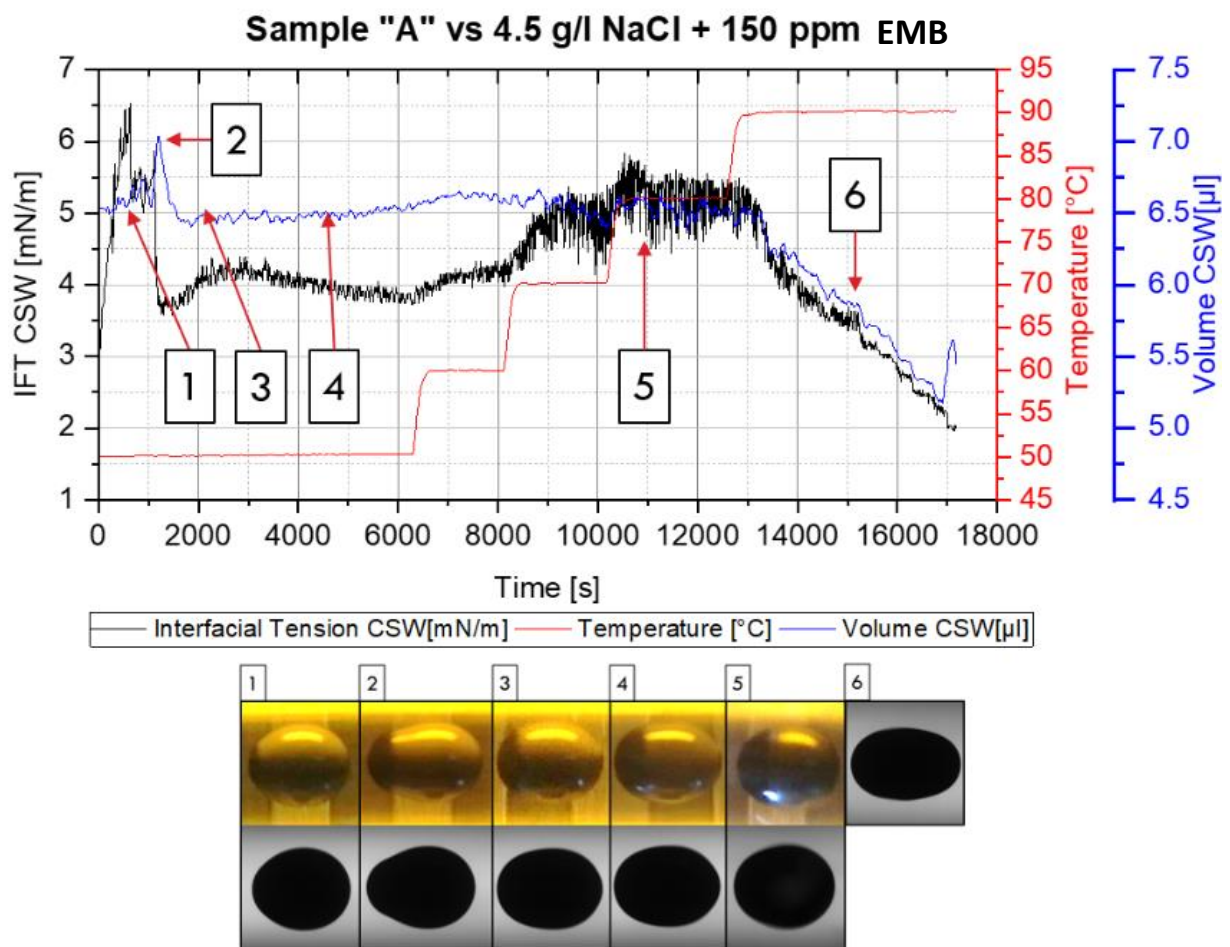


Figure 52. Interfacial tension measurement of Sample A vs 4.8 g/l NaCl and 150 ppm EMB, at 3000 rpm and droplet morphology change during the experiment.

of the droplet, the interface slowly went back to the normal cylindrical shape. From this point and on, the drop shape remained as regular.

Finally, at 90 °C the same demulsification mechanism, as perceived while using 18 ppm EMB but in a more significant magnitude, became evident. A continuous reduction of both IFT and drop volume were observed. The IFT measurement at 90 °C did not achieve stabilization, and no decrement of the reduction rate could be perceived after the allowed measuring time. Even though from the experiments with 150 ppm, one showed a continuous reduction, it will be recommended to perform experiments at 90 °C for extended periods of time. The reduction of IFT could be explained by noticing how the IFT calculation is performed. It involves the drop radius of curvature for the interfacial tension approximation, then the more the drop approached a spherical form the greater the interfacial tension of the system will be. It could be said that at initial stages, the emulsified water induced a drop shape deformation along the “y” axis into a spherical form, as the demulsifier acts on the emulsions, a mass transfer from the oleic phase (emulsified water) to the continuous phase took place. Then without the effect of the emulsions at the interface, the droplet could move away from the spherical form to a more cylindrical shape. The last can be corroborated by the vertical and horizontal drop diameter change over

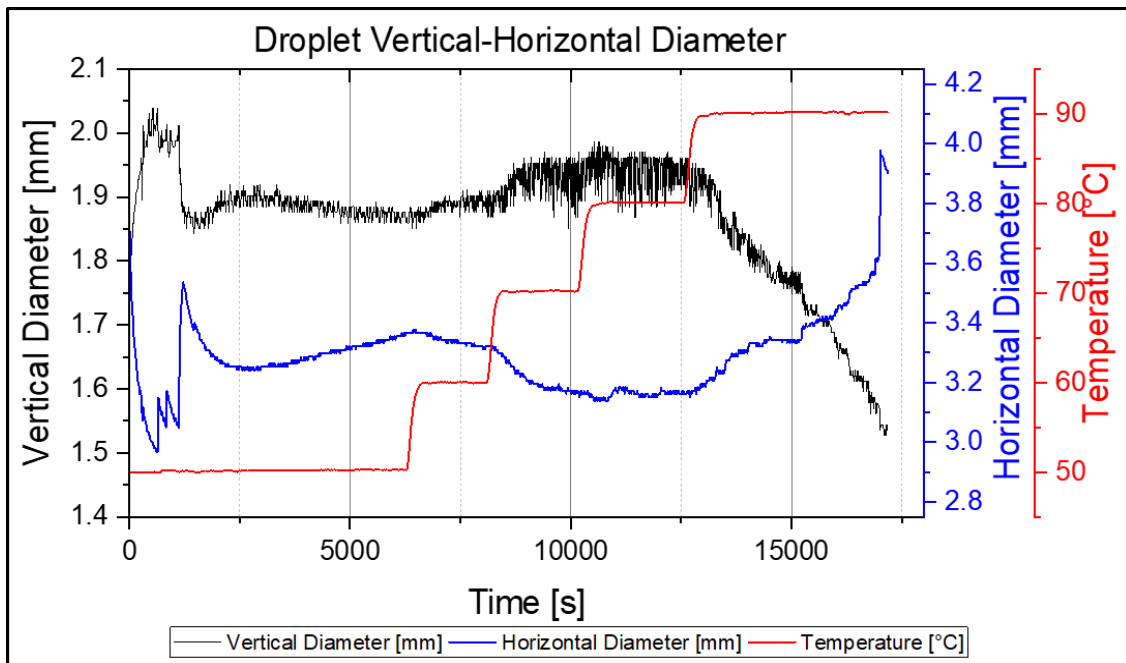


Figure 53. Droplet horizontal and vertical diameter reduction- increment respectively.

the experiment duration showed in Figure 53. Moreover, the drop topology change can be tracked down over time by plotting the alpha parameter or shape factor value vs. time (Figure 54-A), where the shape factor is related to the horizontal and vertical diameter ratio (Figure 54-B).

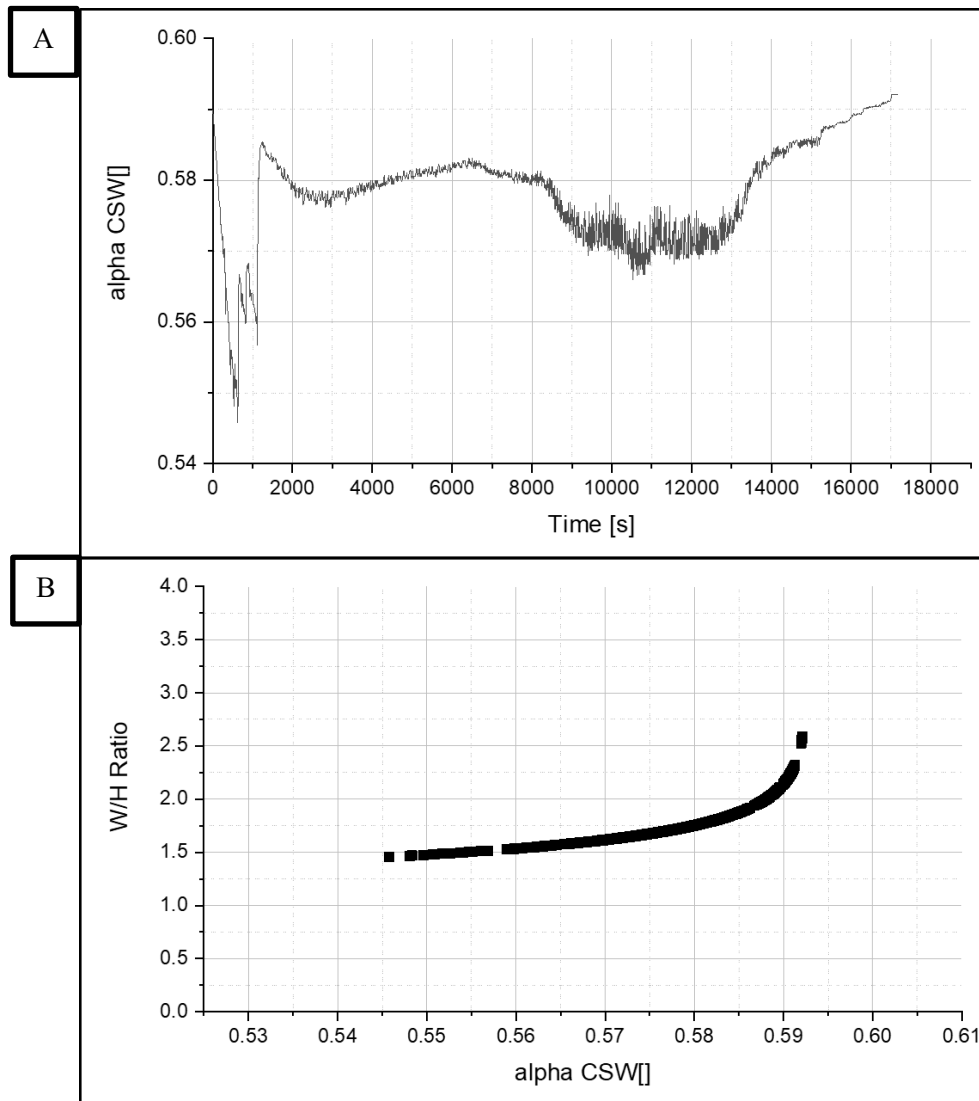


Figure 54. A) Alpha parameter vs time and B) Width-Hight ratio vs. Alpha parameter.

5.3.3 Capillary Number and Sor Reduction

The target of this work was to increase the N_c magnitude, by reducing the interfacial tension orders of magnitude, to reduce the residual oil saturation. In this segment, based on assumptions, it will be reviewed the performance of the emulsion breaker to increase the N_c value.

Applying the eq. 1 for capillary number, and assuming an interstitial velocity of 1 ft/day and a fluid viscosity of 1 cP, it can be calculated the corresponding N_c for two cases:

- A. Oil and brine mimicking the formation salinity – No EMB, IFT = 27 mN/m (90 °C)
- B. Oil and brine containing EMB, IFT = 2.99 mN/m (90 °C)

The capillary number for case A corresponds to $Nc = 1.3 \times 10^{-7}$ and case B to $Nc = 1.18 \times 10^{-6}$. Now the values can be plotted along the capillary desaturation curve from Lake, 1989 for different rock types (Figure 55). For the typical Sandstone desaturation curve, the Nc value lays at the region from which the rock can be desaturated.

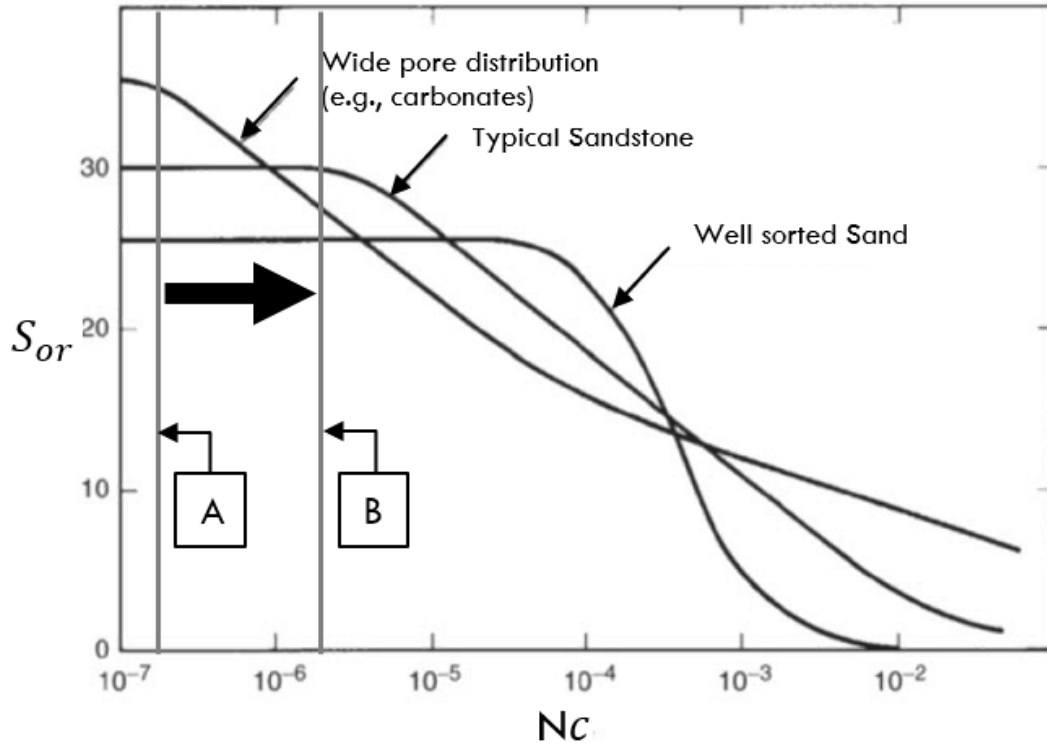


Figure 55. Capillary number of cases A and B (Lake, 1989).

Now the two cases can be compared in Figure 55, line A shows the natural state of the rock-fluid system without the presence of external agents. By the other hand, line B shows the possible outcome of a solution containing EMB, laying at the end of the plateau of typical sandstone desaturation curve. The theoretical increment of the Nc value was found to be one order of magnitude higher as a system containing no demulsifier. It is **imperative** to mention that these results are based on assumptions of rock type and fluid velocities. The actual pore size distribution at the Puchkirchen field will vary; hence, this representation can only be used as a reference. Nevertheless, the brines containing EMB can be further tuned by salinity concentration variation. During this research, the formation water salinity was set as constant 4.5 g/l NaCl, and the EMB concentration gradually increases. As reviewed, salinity can modify the energy between surfactant molecules to a lower or higher state of energy.

Chapter 6

Conclusion, Summary & Future Work

This chapter will summarize the observations during the experiments, and the conclusions taken out of them are given. It is briefly explained what was done along with the project, and the last point concerns the future work that can be performed to enlight the plausibility of emulsion breaker as an EOR agent.

6.1 Conclusion

In this work, a clear fluid separation, of an oleic and aqueous phase, could not be achieved by temperatures in as much as 94°C, without the addition of an emulsion breaker, neither by a centrifugal acceleration of 4400 m/s^2 . It is recommended the use of full sample A (oleic phase containing emulsified water) to observe the effects of the heavy fractions of the oil, such as natural surface-active agents contained in the oleic phase. These components are responsible for the emulsification of the brine that enters in contact with the oil under turbulent conditions.

Sample A was classified as water into oil emulsions which lays in the range of tight emulsions, corroborated by the Microscopy image method. Due to the emulsifying tendency of the Puchkirchen fluids, phase behavior experiments could not be used as a screening tool for finding the optimum salinity or EMB concentration. Hence, the screening of the solutions was performed by experiments involving the Spinning drop Tensiometer.

The salinity concentration showed to have no considerable effect on IFT reduction with brines containing no demulsifier, the last was confirmed by Spinning Drop Tensiometer experiments.

The Alkali performance was found to have a limited action on IFT reduction, possibly due to its low total acid number. The use of Emulsion Breaker not only reduced the IFT of the fluids in a greater magnitude than the alkali solutions but also mitigating the effects of W/O emulsion on IFT measurements (by breaking the emulsions). The last mentioned was proven by Spinning Drop Tensiometer experiments.

Oil droplet morphology deformations were observed during IFT measurements. Ellipsoidal and ballooned droplet shapes appeared under low and high emulsion breaker (EMB) concentrations,

respectively. The ellipsoidal droplet deformation in “y” axis it is hypothesized to be due to the low EMB concentration (18 ppm), which may be unable to break the W/O emulsions efficiently. Then, the remaining emulsions in the oleic phase allocate themselves, by density difference, at the interface oil-brine, generating a pulling effect towards the normal force axis “y”. Then, the ellipsoidal droplet deformation by emulsions is perceived.

Sample A, in combination with brines containing higher emulsion breaker concentrations (75-150 ppm) occasionally leads to short periods of ballooning effect, which disappears as the demulsification process takes place. The brine containing 4500 ppm NaCl and 150 ppm EMB provided the lowest IFT measurements and with fewer variations during measurements. It is recommended to increase the concentration of demulsifier and change the range of salinities to find lower states of interfacial tension for its use in displacing experiments.

The droplet topology deformation into elliptical or ballooning effect appears to be independent of the drop volume. These deformations were observed at different volumes and a variety of emulsion breaker concentration in the combination of temperatures above 50°C. The activation energy is hypothesized to be an enhancement of emulsion breaker action at high temperatures in combination to demulsification mechanisms; such as water drop expansion (decrease of the natural surface-active material in the monolayer coating the droplet). The EMB effect is hypothesized to have a greater diffusion into the interfacial film due to the increase of the kinetic energy as the temperature rises; hence, experiments at ambient conditions have poor performance. Moreover, the effect of EMB on samples that were previously treated at high temperatures (94°C) is still perceived in the demulsification of the water in oil emulsions even after the cooling of the system.

Emulsion breaker proved to reduce the interfacial tension from the natural state of energy of 27 mN/m to an average of 2.99 mN/m at 90 °C. In this research, only fluid-fluid interaction was investigated; hence, the effect of rock-fluid, which might have on oil recovery is still unknown. Then in order to approve or discard the emulsion breaker application as an EOR agent, displacing experiments are needed.

Finally, the focus of this research had been to find an economic methodology to increase oil production. The performance of EMB as an EOR method lays at the envelope of the interfacial tension reduction needed to start the desaturation a rock (in theory). Therefore, it is worth to invest time to improve the solutions targeting to test its performance as displacement fluid.

6.2 Summary

In order to avoid redundancy of the described process during the experimental, discussion, and conclusion, this segment will treat mainly the input and the corresponding output of each Chapter.

This project investigated the application of two EOR methods:

- Alkali by Sodium Carbonate, $NaCO_3$
- Emulsion Breaker by DMO-86102, **EMB**

For it, fluid samples were retrieved from the Field. After separation, by centrifuging, three different oleic phases could be distinguished, from which one must be selected:

- Full sample A, as retrieved from the wellhead containing emulsified water
- Light fraction, an upper light fraction after centrifuging
- Heavy fraction, settled emulsions and heavy oil components

Then, in order to correctly choose a fraction, experiments involving phase behavior of **full sample A**, and **light fraction**, were performed. Meanwhile, the light fraction phase behavior showed a sharp separation of the oil and water phases, the full sample A emulsified the brine that entered in contact with under turbulent conditions. The output of the phase behavior assisted in the selection of full sample A, which was renamed as Sample A during the next set of experiments.

Sample A was characterized by Microscopy image analysis. The output suggested that the emulsions in the system are classified as tight emulsions, based on the droplet size distribution.

The experiments of Phase Behavior and Dynamic Interfacial Tension measurements can be summarized in the following sequence:

1. Blank test, to investigate the natural state of the fluids. For it, a brine that mimics the salinity of the field was used.
2. Salinity and Temperature Effect. Salinity and Temperature were systematically changed. The main idea was to identify the effect of these two variables on the system behavior.
3. Emulsion Breaker. In those experiments involving EMB were performed. Its effect on the IFT reduction and demulsification action was evaluated while varying the demulsifier concentration.

The experiments performed with brines containing EMB led to distortions of the droplet topology and an observation of an enhancement of the demulsifier action when high temperatures were reached (activation energy). The ellipsoidal and ballooning deformation is

theorized to be related to the small and greater EMB concentration, respectively. The activation energy was explained as an enhancement of the demulsifier action by an increase of the diffusion of the demulsifier as the kinetic energy of the system raised.

An average interfacial tension of **2.99 mN/m (± 0.1)** was recorded while using a brine containing 4.5 g/l NaCl and 150 ppm EMB at 90 °C and 3000 rpm. Experiments performed with that solution provided the lowest interfacial tension with less variation between experiments.

6.3 Future Work

Up to now, it has been reviewed the effect of emulsion breaker as IFT reduction agent and as a way to control emulsions in the system simultaneously. Then in order to mark a clear line into the plausibility of the emulsion breaker application as an enhanced oil recovery method, is recommended to test the solutions as the displacing fluid in flooding experiments such as:

- IFT measurements: During the experiments involving the use of demulsifier, the salinity concentration was kept constant. Hence, variations of salinity while keeping the EMB concentration constant may provide further reductions on interfacial energy.
- Microfluidics: To observe the fluid interaction of the brines and the oil as the injected brine displaces the oil under laminar conditions. Microfluidics is an excellent way to investigate the emulsion breaker action into the demulsification of the system under dynamic conditions. In such a case, an oil viscosity reduction due to demulsification can be expected. Consequently, an improvement in the mobility ratio may be achieved.
- Core flooding experiments: The previous experiments shed light on the fluid-fluid interaction, but core flooding experiments will provide the first glance of how the whole system will behave under reservoir conditions.

These displacement methods can bring more light into the possibility of application or discarding of this method.

In addition, further fluid characterization shall be performed to understand the oil composition and clarify the origin of the emulsifying agent contained in the oleic phase, which is believed to be caused by the asphaltenes contained in the oil. A good practice is to perform a SARA test, which uses the principle of Chromatography to dissolve and measure the heavy fractions contained in the oil, such as Saturates, Asphaltenes, Resins, and Aromatics (Ramalho et al., 2010).

Moreover, the emulsions described in this project have great uncertainty regarding the emulsion formation location. Due to they can form in any of the critical mixing points that the fluid

encounters as it makes its journey to the surface, as 1) the formation, 2) the sandface and perforation channels, 3) bottom-hole pump, 4) tubing, 5) choke, 6) and surface equipment (Smit, 1987). Hence, additional sampling measures shall be considered to determine where emulsions are generated; such as bottom hole sampling or reduction of the flow rate prior to the sampling.

Chapter 7

References

- Allen, T. O., & Roberts, A. P. (1989). Surfactants for Well Treatments—Chapter 6. In *Production Operations 2: Well Completions, Workover, and Stimulation*.
- Arnold, P. (2018). *Experimental Investigation of Interfacial Tension for Alkaline Flooding*. Montanuniversität, Leoben.
- Butt, H.-J., Graf, K., & Kappl, M. (2003). *Physics and chemistry of interfaces* (Vol. 138). Wiley Online Library.
- Calmes, J., & Dash, S. (2019, June 15). Dipole Interactions. Brilliant.org. Retrieved from <https://brilliant.org/wiki/dipole-interactions/>
- Calmes, J., Hridoy, R., & Rafael, R. (2019, June 15). Van der Waals Force. Brilliant.org. Retrieved from <https://brilliant.org/wiki/van-der-waals-force/>
- Cayias, J., Schechter, R., & Wade, W. (1975). The measurement of low interfacial tension via the spinning drop technique. *Adsorption at Interfaces*, 8, 234–247.
- Couper, A., Newton, R., & Nunn, C. (1983). A simple derivation of Vonnegut's equation for the determination of interfacial tension by the spinning drop technique. *Colloid and Polymer Science - COLLOID POLYM SCI*, 261, 371–372. <https://doi.org/10.1007/BF01413946>
- DataPhysics. (2013). *Filderstadt, Germany- service@dataphysics-instruments.com*.
- Ese, M.-H., Sjöblom, J., Djuve, J., & Pugh, R. (2000). An atomic force microscopy study of asphaltenes on mica surfaces. Influence of added resins and demulsifiers. *Colloid and Polymer Science*, 278(6), 532–538.

- Gregersen, E. (2019). Surface-active agent. In *Encyclopedia Britannica*. Retrieved from <https://www.britannica.com/science/surfactant>
- Gross, D., Sachsenhofer, R., Rech, A., Sageder, S., Geissler, M., Schnitzer, S., & Troiss, W. (2015). The Trattnach Oil Field in the North Alpine Foreland Basin (Austria). *Austrian Journal of Earth Sciences*.
- Kang, W., Jing, G., Zhang, H., Li, M., & Wu, Z. (2006). Influence of demulsifier on interfacial film between oil and water. *Colloids and Surfaces A: Physicochemical and Engineering Aspects*, 272(1–2), 27–31.
- Krüss. (2019). *Spinning Drop Tensiometer*. Retrieved from www.kruss-scientific.com
- Lake, L. W. (1989). *Enhanced Oil Recovery*. Pearson Education Company.
- Lake, L. W., Fanchi, J. R., Mitchell, R. F., Arnold, K. E., Clegg, J. D., Holstein, E., & Warner, H. R. (2006a). Chapter 12. Crude Oil Emulsions. In *Petroleum Engineering Handbook—Vol. 1 General Engineering*. Society of Petroleum Engineers.
- Lake, L. W., Fanchi, J. R., Mitchell, R. F., Arnold, K. E., Clegg, J. D., Holstein, E., & Warner, H. R. (2006b). Chapter 19—Crude Oil Emulsions. In *Petroleum Engineering Handbook—Vol. 1 General Engineering*. Society of Petroleum Engineers.
- Lyons, W. C., & Plisga, G. J. (2011). Chapter 5—Reservoir Engineering. In *Standard handbook of petroleum and natural gas engineering*. Elsevier.
- Mohammed, R., Bailey, A., Luckham, P., & Taylor, S. (1993). Dewatering of crude oil emulsions 2. Interfacial properties of the asphaltic constituents of crude oil. *Colloids and Surfaces A: Physicochemical and Engineering Aspects*, 80(2–3), 237–242.
- Morrow, N. R., Ma, S., Zhou, X., & Zhang, X. (2017). Characterization of Wettability from Spontaneous Imbibition Measurements. *Western Research Institute - University of Wyoming*.
- Myers, D. (2005a). Fluid Surfaces and Interfaces. In *Surfactant science and technology*. John Wiley & Sons.
- Myers, D. (2005b). *Surfactant science and technology*. John Wiley & Sons.

- Ott, H. (2018a). *Enhanced Oil Recovery—Course notes*. Presented at the Montanuniversity, Leoben. Montanuniversity, Leoben.
- Ott, H. (2018b). *Surfactants at the Interface—Course notes*. Presented at the Montanuniversity, Leoben. Montanuniversity, Leoben.
- Ramalho, J. B. V., Lechuga, F. C., & Lucas, E. F. (2010). Effect of the structure of commercial poly (ethylene oxide-b-propylene oxide) demulsifier bases on the demulsification of water-in-crude oil emulsions: Elucidation of the demulsification mechanism. *Quimica Nova*, 33(8), 1664–1670.
- Rohöl-Aufsuchungs Aktiengesellschaft (RAG). (2013, October). *75 years of successful energy production (Zistersdorf)*.
- Schorling, P.-C., Kessel, D., & Rahimian, I. (1999). Influence of the crude oil resin/asphaltene ratio on the stability of oil/water emulsions. *Colloids and Surfaces A: Physicochemical and Engineering Aspects*, 152(1–2), 95–102.
- Shah, D. O. (2012). *Improved oil recovery by surfactant and polymer flooding*. Elsevier.
- Sheng, J. J. (2013a). Alkaline Flooding. In *Enhanced Oil Recovery Field Case Studies*.
- Sheng, J. J. (2013b). Polymer Flooding-Fundamentals and Field Cases. In *Enhanced Oil Recovery Field Case Studies*.
- Sheng, J. J. (2013c). Water-Based EOR in Carbonates and Sandstones: New Chemical Understanding of the EOR Potential Using “Smart Water.” In *Enhanced Oil Recovery Field Case Studies*.
- Smit, H. V. (1987). Crude Oil Emulsions. In *Petroleum Engineering Handbook*.